

Electronic Supplementary Information

Controlling supramolecular copolymerization of alkynylplatinum(II) terpyridine complexes: from isodesmic to cooperative mechanisms

Sehee Kim,^{a,b} Minhye Kim,^{a,b} Seojeong Woo,^a Juyeong Kim,^a Sung Ho Jung*^a and Jong Hwa Jung*^a

^aDepartment of Chemistry and Research Institute of Natural Sciences Gyeongsang National University, Jinju 52828, Korea

^bThese authors contributed equally.

Contents

1. Method

1.1 General characterization	S3
1.2 UV-vis studies	S3
1.3 Circular Dichroism (CD) studies	S3
1.4 Polymerization of supramolecular polymers by UV irradiation with Hg lamp	S3
1.5 SEM observation	S3
1.6 TEM observation	S4
1.7 Calculation of thermodynamic parameter	S4

2. Synthesis and characterization

2.1 Synthesis of 2	S4
2.2 Synthesis of 3	S5
2.3 Synthesis of 4	S5
2.4 Synthesis of 5	S6
2.5 Synthesis of Pt-Sat-C18	S6
2.6 Synthesis of 6	S7
2.7 Synthesis of Pt-DA-C25	S7

3. Supplementary scheme and figures

3.1 Scheme S1	S8
3.2 Figures S1-S28	S9
3.3 Tables S1-S6	S25

4. Analytical data

4.1 ¹ H- and ¹³ C-NMR spectra	S27
4.2 ESI-MS spectra	S34

Supplementary data

1. Methods

1.1 General characterization: The ^1H and ^{13}C NMR spectra were taken on a Bruker DRX 300, and Bruker DRX 500. Mass spectroscopy samples were analyzed on a JEOL JMS-700 mass spectrometer. The high resolution mass spectra (HR-MS) were measured by electrospray ionization (ESI) with a micro TOF Focus spectrometer from SYNAPT G2 (Waters, U.K.). IR spectra were observed over the range $500\text{-}4000\text{ cm}^{-1}$, with a Thermo scientific Nicolet iS 10 instrument.

1.2 UV-vis studies: The UV-vis spectra were recorded on a JASCO V-750 UV-visible spectrophotometer. The UV-vis spectra were determined over the range of $200\text{-}800\text{ nm}$ using a quartz cell with 1.0 and 10 mm path length. Scans were taken at rate of 400 nm/min with a sampling interval of 1 nm and response time of 0.5 s . To elucidate the supramolecular polymerization process, **Pt-Sat-C18** and **Pt-DA-C25** were dissolved in DMSO/ H_2O ($5:1\text{ v/v}$). After adding the sample to the UV cells, it was heated to 363 K (1 K/min) to form the monomeric species in UV-vis spectroscopy. Then the sample was cooled to 293 K (1 K/min) in UV-vis spectroscopy.

1.3 Circular Dichroism (CD) Studies: The CD spectra were recorded on a Jasco J-815 CD spectrophotometer. CD spectra were determined over the range of $200\text{-}800\text{ nm}$ using a quartz cell with 1.0 and 10 mm path length. Scans were taken at rate of 400 nm/min with a sampling interval of 1 nm and response time of 0.5 s . The scans were acquired for the supramolecular nanostructure directly at 293 K .

1.4 Polymerization of supramolecular polymers by UV irradiation with Hg lamp: Polymerization of the supramolecular polymer ($300\text{ }\mu\text{M}$) by UV irradiation was carried out in a quartz cell (length 80 mm , inner diameter 10 mm , wall thickness 0.1 mm) using a 50 mV Hg lamp (254 nm) by changing irradiation times. The distance between the samples and Hg lamp was 10 cm . The photoreactor was maintained at $25\text{ }^\circ\text{C}$ during UV-irradiation. Then, conversion of the supramolecular homo and copolymers was observed by FT-Raman (a Bruker FRS-100S).

1.5 SEM observation: FE-SEM images were observed using a JEOL (JSM-7900F). The images of samples using an accelerating voltage 10 kV and an emission current of $8\text{ }\mu\text{A}$.

Samples were prepared by dropping dilute solution of supramolecular nanostructure formed in water on glasses following by spinning, drying and coating them with a thin layer of Pt to increase the contrast.

1.6 TEM observation: The TEM images were observed using a Thermo Fisher Scientific Talos L120C. The samples of supramolecular nanostructure were placed on a carbon coated copper grids (200 mesh), which were negatively stained with uranyl acetate.

1.7 Calculation of thermodynamic parameter: The thermodynamic parameters governing the supramolecular polymers of **Pt-DA-C25** and co-assembled polymers formed at various composition ratios of **Pt-Sat-C18** and **Pt-DA-C25** were obtained by the global fitting of the cooling curves, respectively. This global fitting is performed by using the equilibrium (EQ) model reported by ten Eikelder and coworkers.¹ The values for the elongation enthalpy (ΔH_e) and the entropy (ΔS_e), and elongation binding constant (K_e) used in the cooperative supramolecular polymerization models were determined by the global fitting of the cooling curves,²⁻⁴ which were obtained by plotting the degree of aggregation (α_{agg}) of **Pt-Sat-C18** and co-assembled polymers formed at various composition ratios of **Pt-Sat-C18** and **Pt-DA-C25** at 270 nm against temperature with cooling experiments. An elongation binding constant (K_e) for aggregation at 298 K was estimated according to equation 1, from which the enthalpy change (ΔH), and the entropy change (ΔS) were determined:

$$K_e = e^{-\frac{(\Delta H_e - T\Delta S)}{RT}} \quad (\text{equation 1})$$

2. Synthesis and characterization

Unless otherwise noted, chemical reagents and solvents were purchased from commercial suppliers (Tokyo Chemical Industry (TCI), Sigma Aldrich) and used without further purification.

2.1 Synthesis of 2: In a 50 mL round-bottom flask KOH (1.05 g, 18.7 mmol, 5 equiv.) was dissolved in distilled DMSO (20 mL) for 1 hour at 60°C. (*S*)-(+)-2-amino-1-propanol (0.34 g, 4.49 mmol, 1.2 equiv.) was added to a stirred suspension. After 30 min, 4'-chloro-2,2':6',2''-terpyridine (1.00 g, 3.7 mmol, 1 equiv.) was added to the mixture. The reaction mixture was stirred for 4h at 70°C. After 4 hours, The reaction mixture was transferred into a separatory

funnel and washed with DCM and water. The organic phase was dried over Sodium sulfate and solvents were filtered and removed under reduced pressure. The crude product was purified by Al₂O₃ column chromatography (gradient elution DCM/MeOH 100:1 v/v to DCM/MeOH 10:1 v/v) to give **2** (0.96 g, 84%); IR (ATR): 3375, 2926, 2854, 1552, 1468, 1439, 1403, 1353, 1202, 1033, 841, 795, 746, 657, 623 cm⁻¹; ¹H NMR (300 MHz, DMSO-*d*₆) δ 8.71 (ddd, *J* = 4.7, 1.8, 0.9 Hz, 2H), 8.61 (dt, *J* = 8.0, 1.1 Hz, 2H), 8.05 – 7.94 (m, 4H), 7.50 (ddd, *J* = 7.5, 4.8, 1.3 Hz, 2H), 4.09 – 3.91 (m, 2H), 3.23 (q, *J* = 6.3 Hz, 1H), 2.08 (s, 2H), 1.12 (d, *J* = 6.4 Hz, 3H); ¹³C NMR (125 MHz, DMSO-*d*₆) δ 167.2, 157.1, 155.3, 149.7, 137.9, 125.0, 121.3, 107.3, 75.1, 46.2, 20.43; ESI-MS: *m/z* = 307.25 [M+H]⁺ (calculated 306.37 for C₁₈H₁₈N₄O).

2.2 Synthesis of 3: In a 100 mL round-bottom flask was charged with Stearoyl chloride (0.88 mL, 2.6 mmol, 1.3 equiv.) and **2** (0.61 g, 2.0 mmol, 1 equiv.) dissolved in distilled dichloromethane (10 mL). (Triethyl)amine (1.81 mL, 13.0 mmol, 6.5 equiv.) was added by using an ice bath and the reaction mixture was stirred. The reaction mixture was extracted with DCM and water when all starting material was consumed. The organic phase was dried over Sodium sulfate and solvents were filtered and removed under reduced pressure. The crude product was purified by Al₂O₃ column chromatography (DCM/MeOH 100:1 v/v). The product was purified by recrystallization with DCM and ether to give **3** (0.85 g, 74%); IR (ATR): 3287, 2916, 2847, 2360, 1727, 1637, 1562, 1534, 1405, 1361, 1036, 791, 730, 621 cm⁻¹; ¹H NMR (300 MHz, DMSO-*d*₆) δ 8.71 (ddd, *J* = 4.8, 1.8, 0.9 Hz, 2H), 8.61 (dt, *J* = 8.0, 1.1 Hz, 2H), 8.04 – 7.95 (m, 4H), 7.89 (d, *J* = 7.5 Hz, 1H), 7.49 (ddd, *J* = 7.5, 4.8, 1.2 Hz, 2H), 4.22 (t, *J* = 6.1 Hz, 1H), 4.15 (d, *J* = 5.1 Hz, 2H), 2.06 (t, *J* = 7.0 Hz, 2H), 1.46 (s, 2H), 1.26 – 1.06 (m, 31H), 0.89 – 0.79 (t, 3H); ¹³C NMR (125 MHz, CDCl₃) δ 172.69, 166.90, 157.24, 155.92, 149.05, 136.86, 123.94, 121.36, 107.28, 70.79, 44.25, 36.95, 31.93, 29.70, 29.63, 29.50, 29.37, 29.28, 25.77, 22.70, 17.65, 14.13; ESI-MS: *m/z* = 573.42 [M+H]⁺ (calculated 572.84 for C₃₆H₅₂N₄O₂).

2.3 Synthesis of 4: In a 100 mL round-bottom flask Dichloro (1,5-cyclooctadiene) platinum (II) (0.42 g, 1.1 mmol, 1.3 equiv.) and **3** (0.50 g, 0.9 mmol, 1 equiv.) were dissolved in distilled MeOH (20 mL). The reaction mixture was stirred at 90 °C and refluxed until **3** was consumed (ca. 2 – 3 hours). the reaction mixture was filtered with MeOH. The product was purified by recrystallization with MeOH and ether to give **4** (0.65 g, 93%); IR (ATR): 3390, 2916, 2849, 2360, 1608, 1553, 1431, 1223, 1043, 782, 718, 626 cm⁻¹; ¹H NMR (300 MHz, CDCl₃) δ 9.10 – 9.05 (m, 2H), 9.03 (d, *J* = 8.0 Hz, 2H), 8.61 (s, 2H), 8.37 – 8.30 (m, 2H), 8.28 (d, *J* = 9.2 Hz,

1H), 7.71 (t, $J = 6.7$ Hz, 2H), 5.21 (dd, $J = 11.5, 8.8$ Hz, 1H), 4.61 (s, 1H), 4.43 (dd, $J = 11.4, 4.1$ Hz, 1H), 2.22 – 1.94 (m, 2H), 1.40 (d, $J = 6.9$ Hz, 4H), 1.25 (s, 19H), 1.08 (d, $J = 13.6$ Hz, 11H), 0.91 – 0.83 (t, 3H); ^{13}C NMR (125 MHz, CDCl_3) δ 172.65, 169.53, 158.51, 155.70, 151.49, 142.94, 129.72, 126.33, 111.45, 73.39, 44.02, 25.94, 31.76, 29.53, 29.52, 29.48, 29.34, 29.18, 29.15, 25.75, 22.57, 17.45, 14.43; ESI-MS: $m/z = 803.42$ $[\text{M}+\text{H}]^+$ (calculated 803.37 for $\text{C}_{36}\text{H}_{52}\text{ClN}_4\text{O}_2\text{Pt}$).

2.4 Synthesis of 5: In a 100 mL round-bottom flask 30mL of sodium hydroxide (0.07 g, 1.7 mmol, 1 equiv.) was added and 3-ethyleniline (0.18 mL, 1.7 mmol, 1 equiv.) was added. A hexane solution (30 mL), containing stearoyl chloride (0.50 g, 1.7 mmol, 1 equiv.) was slowly added and the reaction mixture was stirred for 4 to 5 hours. After the reaction was completed, the water layer was filtered. The organic phase was removed under reduced pressure using the organic phase as a solvent. The crude product was washed with isopropanol to give **5** (0.50 g, 80%); IR (ATR): 3286, 2914, 2847, 1660, 1603, 1535, 1472, 1462, 1405, 1297, 883 cm^{-1} ; ^1H NMR (300 MHz, CDCl_3) δ 7.62 (s, 1H), 7.56 (d, $J = 7.7$ Hz, 1H), 7.28 (d, $J = 7.7$ Hz, 1H), 7.25 – 7.20 (m, 1H), 7.09 (s, 1H), 3.06 (s, 1H), 2.35 (t, $J = 7.5$ Hz, 2H), 1.78 – 1.67 (m, 2H), 1.25 (s, 30H), 0.92 – 0.83 (t, 3H); ^{13}C NMR (75 MHz, CDCl_3) δ 171.11, 137.66, 128.75, 127.60, 122.79, 122.54, 119.98, 82.86, 37.56, 31.66, 29.43, 29.39, 29.34, 29.20, 29.10, 28.98, 25.28, 22.43, 13.86; ESI-MS: $m/z = 384.42$ $[\text{M}+\text{H}]^+$ (calculated 383.62 for $\text{C}_{26}\text{H}_{41}\text{NO}$).

2.5 Synthesis of Pt-Sat-C18 : In a 100 mL round-bottom flask **5** (0.60 g, 1.6 mmol, 2.5 equiv.) and **4** (0.50 g, 0.6 mmol, 1 equiv.) were dissolved in distilled DCM (20 mL). Diisopropylamine (0.5 mL) and copper iodide (10 mg) were added. The reaction mixture was stirred in the dark for 17 hours. The reaction mixture was extracted with DCM and water. The organic phase was dried over Sodium sulfate and solvents were filtered and removed under reduced pressure. The crude product was purified by Al_2O_3 column chromatography (MeOH/Chloroform 3:100 v/v) to give **Pt-Sat-C18** (0.44 g, 62%); IR (ATR): 3445, 3265, 2152, 1654, 1437, 1405, 1313, 1082, 1018, 952, 707 cm^{-1} ; ^1H NMR (300 MHz, CDCl_3) δ 9.45 (s, 1H), 8.49 (d, $J = 8.1$ Hz, 4H), 8.06 (t, $J = 7.9$ Hz, 2H), 7.99 (s, 2H), 7.84 (d, $J = 8.0$ Hz, 1H), 7.47 (d, $J = 11.9$ Hz, 2H), 7.19 (t, $J = 7.9$ Hz, 2H), 6.80 (d, $J = 7.8$ Hz, 1H), 4.91 (s, 1H), 4.51 (s, 1H), 4.39 (s, 1H), 4.12 (s, 1H), 2.60 (d, $J = 6.5$ Hz, 3H), 2.35 – 2.15 (m, 2H), 2.02 (d, $J = 3.9$ Hz, 3H), 1.82 (q, $J = 7.4$ Hz, 3H), 1.50 – 1.44 (m, 8H), 1.29 (tt, $J = 10.2, 6.1$ Hz, 93H), 0.94 – 0.85 (m, 17H); ^{13}C NMR (75 MHz, CDCl_3) δ 173.88, 173.26, 169.76, 159.14, 155.13, 153.53, 141.43, 139.99, 129.19, 128.99, 126.38, 124.18, 119.66, 111.68, 97.51, 74.03, 61.78,

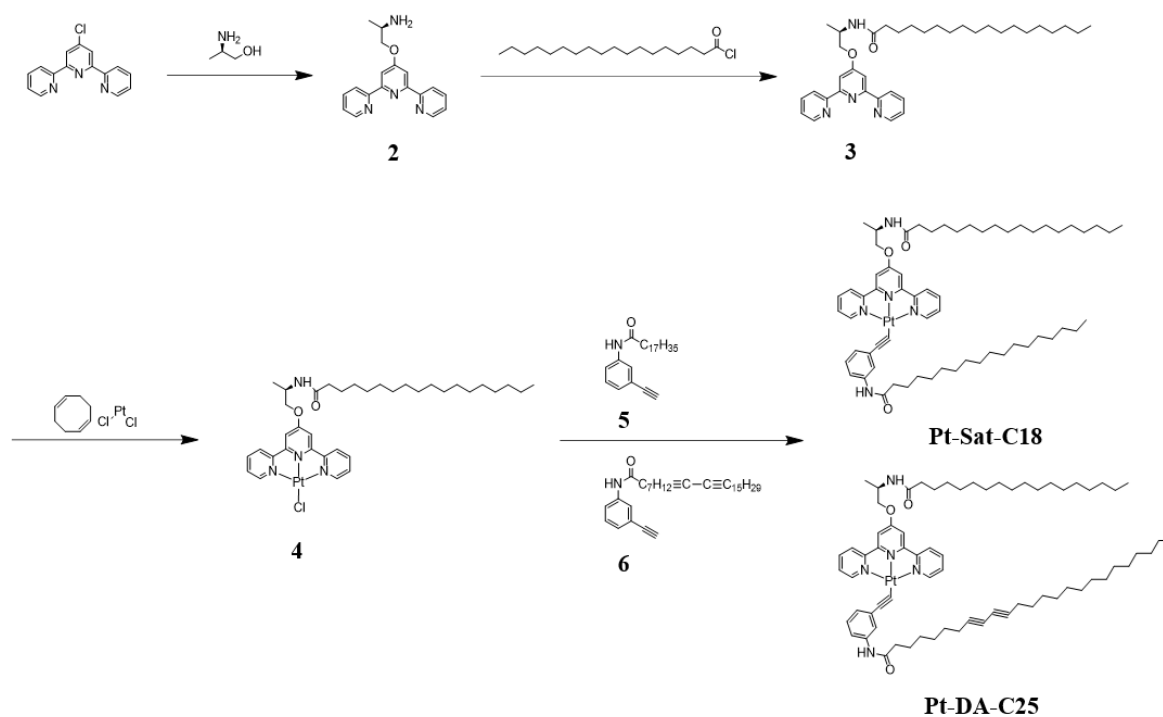
44.77, 37.86, 37.42, 37.06, 33.12, 32.13, 30.24, 29.98, 29.92, 29.89, 29.86, 29.74, 29.69, 29.51, 29.43, 28.28, 27.31, 26.32, 26.10, 22.81, 21.54, 19.91, 17.70, 14.06, 14.04; ESI-MS: $m/z = 1150.25 [M]^+$ (calculated 1150.53 for $C_{62}H_{92}N_5O_3Pt$).

2.6 Synthesis of 6: In a 100 mL round-bottom flask 10,12-Pentacosadiynoic Acid (0.50 g, 1.3 mmol, 1 equiv.) was dissolved in Dichloromethane (20 mL). (It proceeded in the dark.) Thionyl chloride (1.00 mL, 13.8 mmol, 5.2 equiv.) was added as dropwise and refluxed at 50°C for 3 hours. The solvent and Thionyl chlorid removed under reduced pressure. The obtained product and 3-Ethynylaniline (0.28 mL, 2.6 mmol, 2 equiv.) were dissolved in Tetrahydrofuran (20 mL). After adding TEA (1 mL) at 0°C, it was stirred at room temperature. The reaction mixture was extracted with DCM and water. The organic phase was dried over Sodium sulfate and solvents were filtered and removed under reduced pressure. The product was purified by recrystallization with MeOH to give **6** (0.53 g, 83%); IR (ATR): 3278, 2916, 2846, 1651, 1583, 1536, 1464, 1464, 1421, 1407, 1248, 1185, 792, 720, 684 cm^{-1} ; 1H NMR (300 MHz, $CDCl_3$) δ 7.63 (s, 1H), 7.56 (d, $J = 7.9$ Hz, 1H), 7.29 (d, $J = 7.7$ Hz, 1H), 7.25 – 7.20 (m, 1H), 7.07 (s, 1H), 3.06 (s, 1H), 2.35 (t, $J = 7.5$ Hz, 2H), 2.24 (d, $J = 13.4$ Hz, 4H), 1.71 (q, $J = 7.3$ Hz, 2H), 1.53 (dd, $J = 15.8, 8.4$ Hz, 5H), 1.26 (s, 29H), 0.90 – 0.85 (t, 3H); ^{13}C NMR (75 MHz, $CDCl_3$) δ 171.47, 138.08, 129.18, 128.03, 123.22, 122.97, 120.40, 83.28, 65.46, 65.37, 37.93, 32.07, 29.80, 29.78, 29.76, 29.63, 29.50, 29.29, 29.25, 29.01, 28.88, 28.50, 28.41, 25.62, 22.84, 19.36, 19.33, 14.28; ESI-MS: $m/z = 474.25 [M+H]^+$ (calculated 473.75 for $C_{33}H_{47}NO$).

2.7 Synthesis of Pt-DA-C25 : In a 100 mL round-bottom flask **6** (0.47 g, 1.0 mmol, 1.6 equiv.) and **4** (0.50 g, 0.6 mmol, 1 equiv.) were dissolved in distilled DCM (25 mL). Diisopropylamine (0.5 mL) and copper iodide (10 mg) were added. The reaction mixture was stirred in the dark for 15 hours. The reaction mixture was extracted with DCM and water. The organic phase was dried over Sodium sulfate and solvents were filtered and removed under reduced pressure. The crude product was purified by Al_2O_3 column chromatography (DCM/MeOH 100:1 v/v) to give **Pt-DA-C25** (0.46 g, 59%); IR (ATR): 3356, 3233, 2150, 2046, 1982, 1653, 1315, 1084, 1019, 952, 706 cm^{-1} ; 1H NMR (300 MHz, THF- d_8) δ 10.63 (s, 1H), 8.61 (d, $J = 7.9$ Hz, 2H), 8.40 (s, 2H), 8.27 (s, 1H), 8.11 (d, $J = 8.2$ Hz, 1H), 8.03 (d, $J = 10.9$ Hz, 4H), 7.66 (s, 1H), 7.52 (t, $J = 6.7$ Hz, 2H), 7.10 (t, $J = 7.9$ Hz, 1H), 6.72 (d, $J = 7.6$ Hz, 1H), 4.60 (s, 1H), 4.35 (s, 1H), 4.19 (s, 1H), 2.61 (t, $J = 7.4$ Hz, 2H), 1.63 – 1.41 (m, 18H), 1.30 (t, $J = 3.1$ Hz, 56H), 0.93 – 0.86 (t, 6H); ^{13}C NMR (75 MHz, THF- d_8) δ 173.62, 172.56, 170.25, 159.41, 155.78, 154.18, 142.35, 141.28, 130.12, 128.92, 127.25, 124.30, 118.99, 112.10, 103.05, 77.63, 77.49, 66.69, 66.49,

62.61, 45.17, 37.95, 37.18, 32.65, 30.57, 30.52, 30.48, 30.45, 30.39, 30.37, 30.34, 30.29, 30.23, 30.13, 30.04, 30.02, 29.99, 29.92, 29.84, 29.79, 29.63, 29.49, 29.36, 26.70, 26.52, 24.67, 23.27, 21.55, 19.71, 19.64, 17.94, 14.11, 14.09; ESI-MS: $m/z = 1240.75 [M]^+$ (calculated 1240.66 for $C_{69}H_{98}N_5O_3Pt$).

3. Supplementary scheme and figures



Scheme S1. Synthetic routes of **Pt-Sat-C18** and **Pt-DA-C25**.

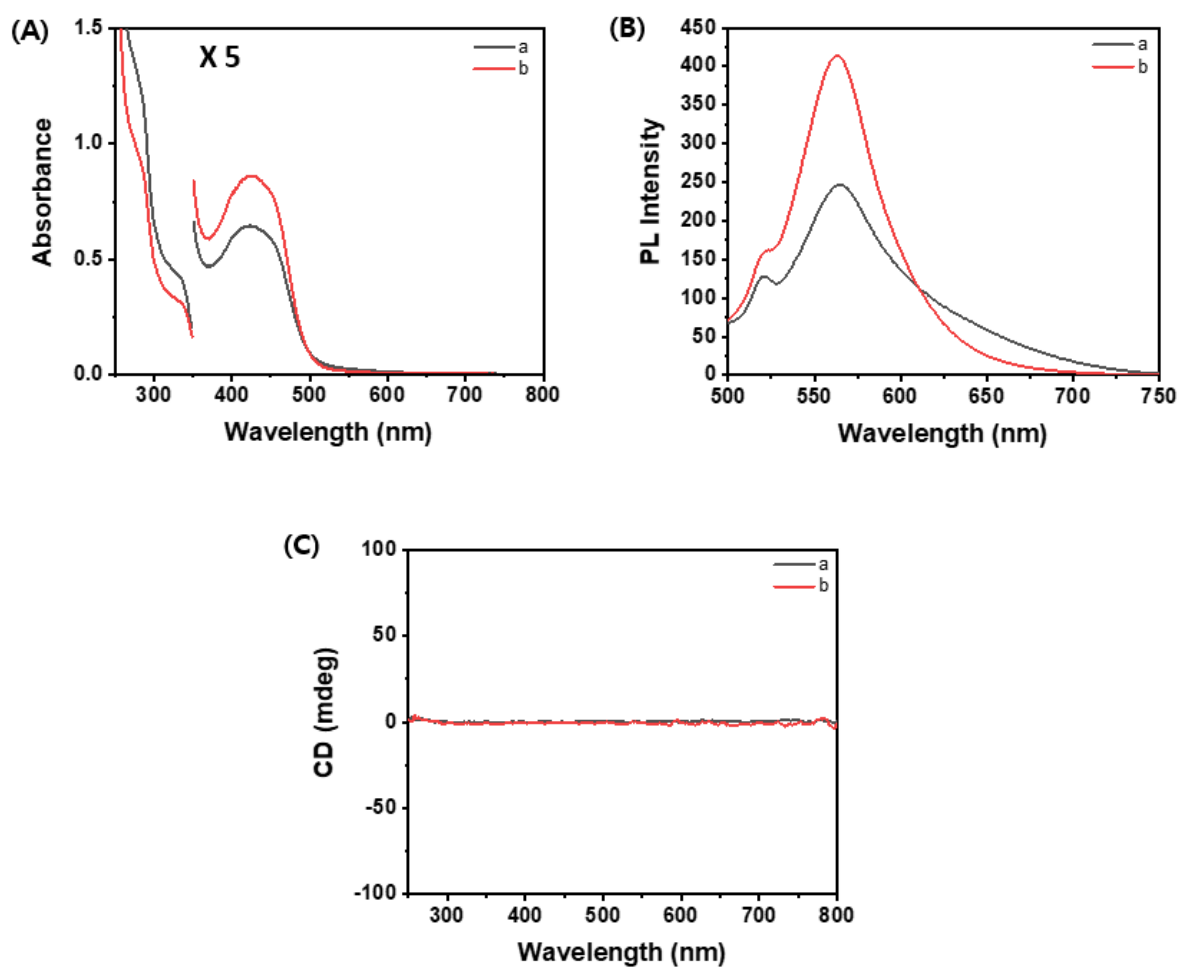


Fig. S1 (A) UV-vis, (B) PL and (C) CD spectra of (a) **Pt-Sat-C18** (300 μ M) and (b) **Pt-DA-C25** (300 μ M) in pure DMSO at 293 K.

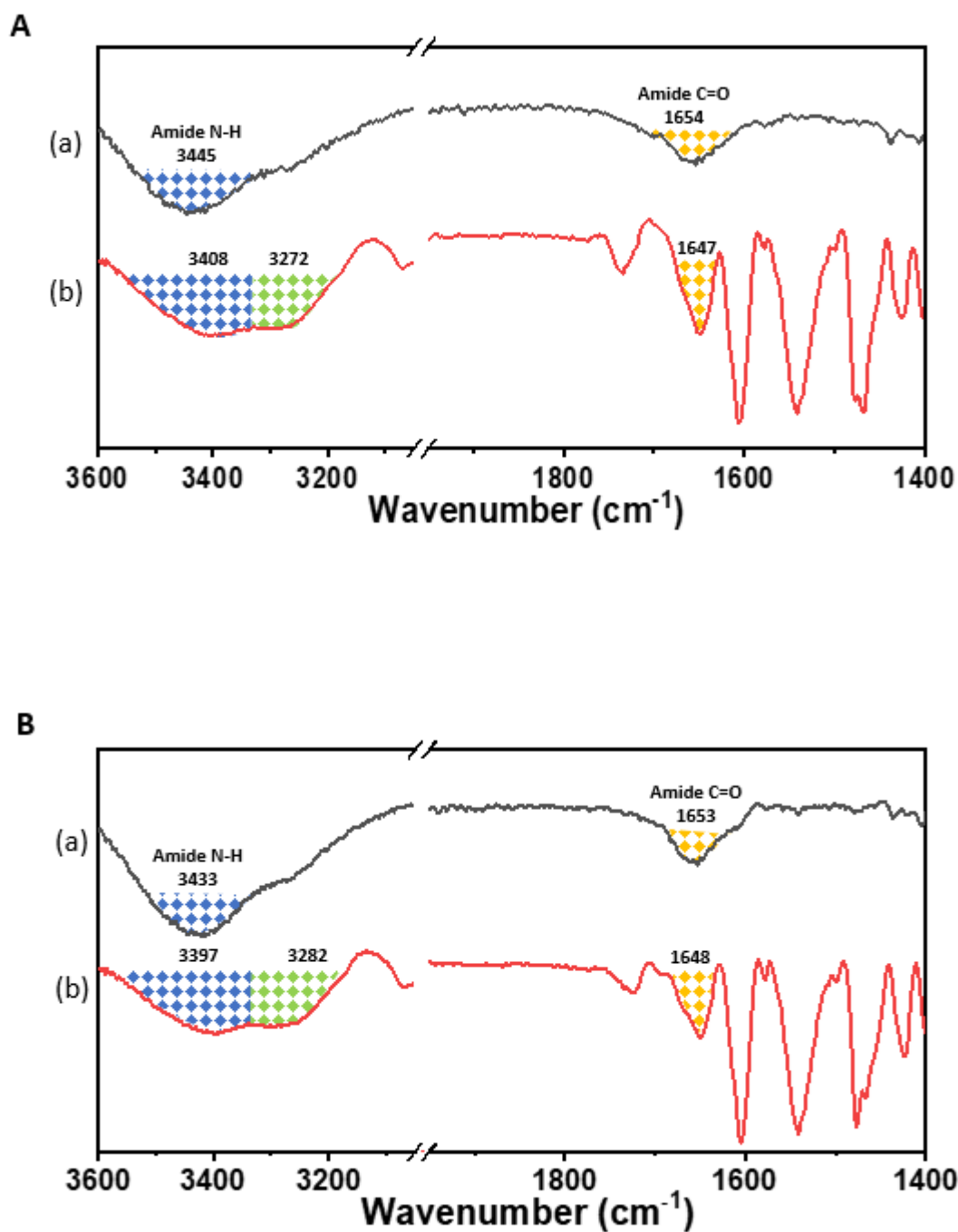


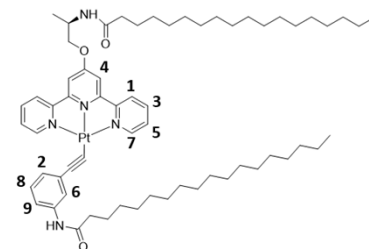
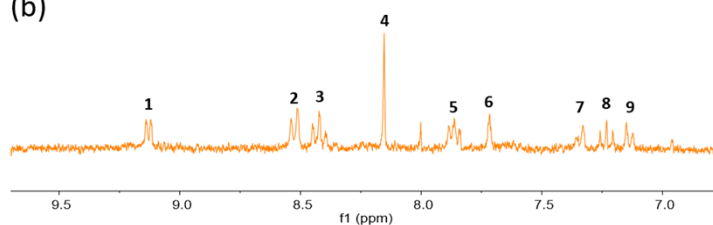
Fig. S2 FT-IR spectra of (A) **Pt-Sat-C18** (1 mM) in (a) pure DMSO and (b) a mixture of DMSO and H_2O (5:1 v/v). (B) **Pt-DA-C25** (1 mM) in (a) pure DMSO and (b) a mixture of DMSO and H_2O (5:1 v/v).

A

(a)



(b)

**B**

(a)



(b)

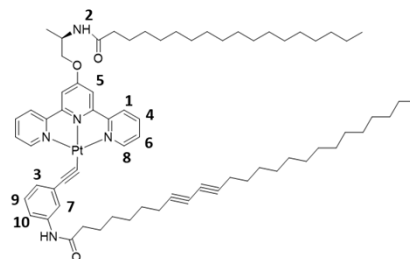
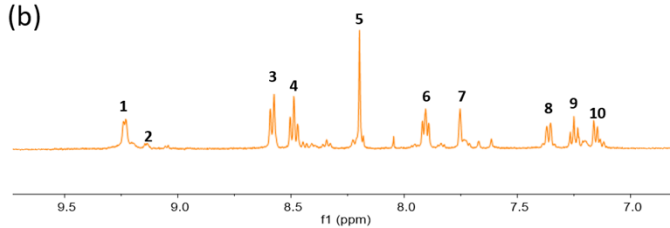


Fig. S3 ^1H NMR spectra of (A) **Pt-Sat-C18** (5 mM) in a mixture of $\text{DMSO-}d_6/\text{D}_2\text{O}$ 5:1 v/v at (a) 298 K and (b) 363 K. (B) **Pt-DA-C25** (5 mM) in a mixture of $\text{DMSO-}d_6/\text{D}_2\text{O}$ (5:1 v/v) at (a) 298 K and (b) 363 K.

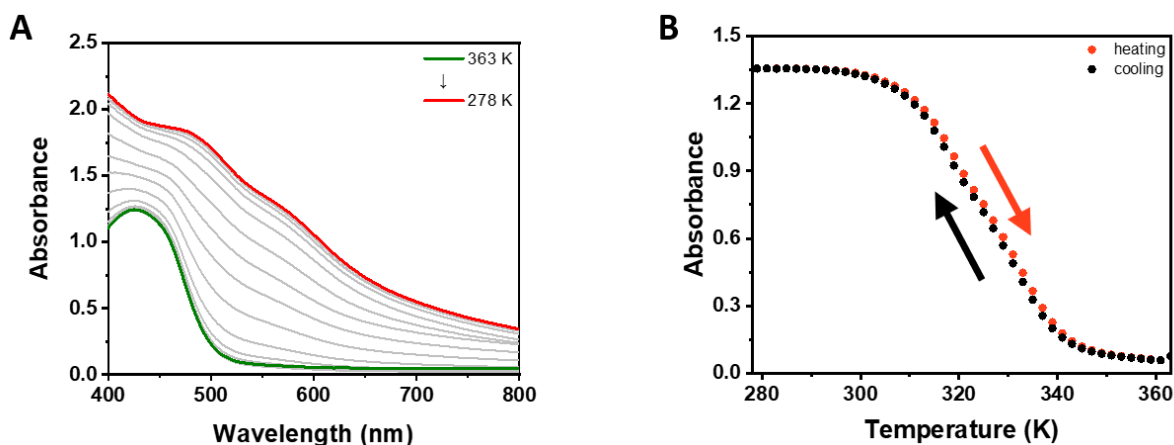


Fig. S4 (A) Temperature-dependent UV-Vis spectral changes of **Pt-Sat-C18** (300 μM) upon heating and cooling at a rate of 1 K min^{-1} in a mixture of DMSO and H_2O (5:1 v/v). (B) Plots for absorbances vs. temperatures of **Pt-Sat-C18** at 550 nm.

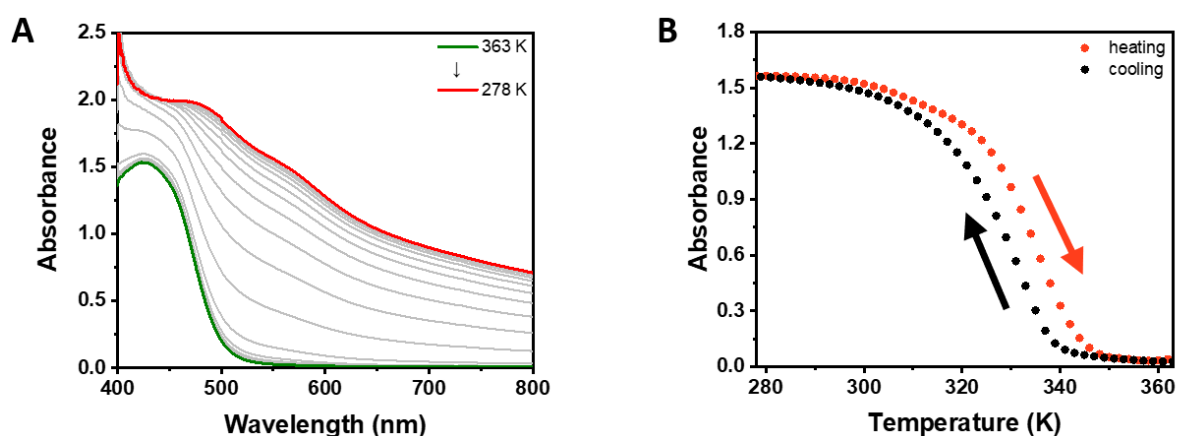


Fig. S5 (A) Temperature-dependent UV-Vis spectral changes of **Pt-DA-C25** (300 μM) upon heating and cooling at a rate of 1 K min^{-1} in a mixture of DMSO and H_2O (5:1 v/v). (B) Plots for absorbances vs. temperatures of **Pt-DA-C25** at 550 nm.

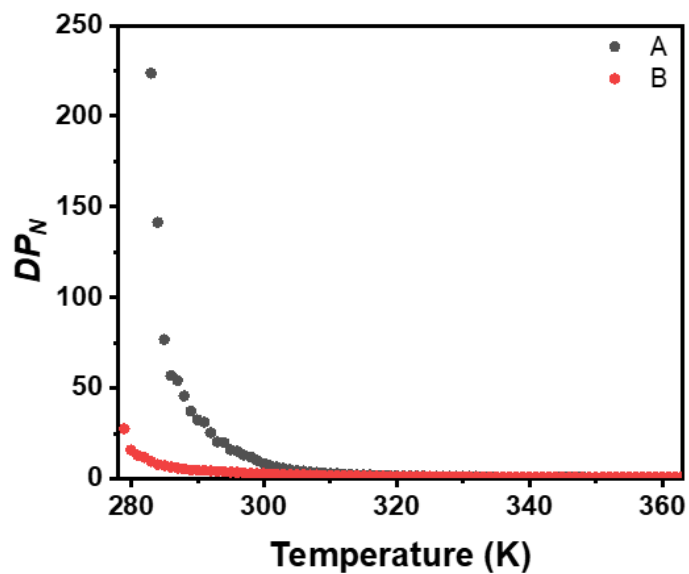


Fig. S6 Plots for DP_N vs. temperatures of (A) **Pt-Sat-C18** and (B) **Pt-DA-C25** upon cooling at a rate of 1 K min^{-1} in DMSO and H_2O (5:1 v/v) at 270 nm.

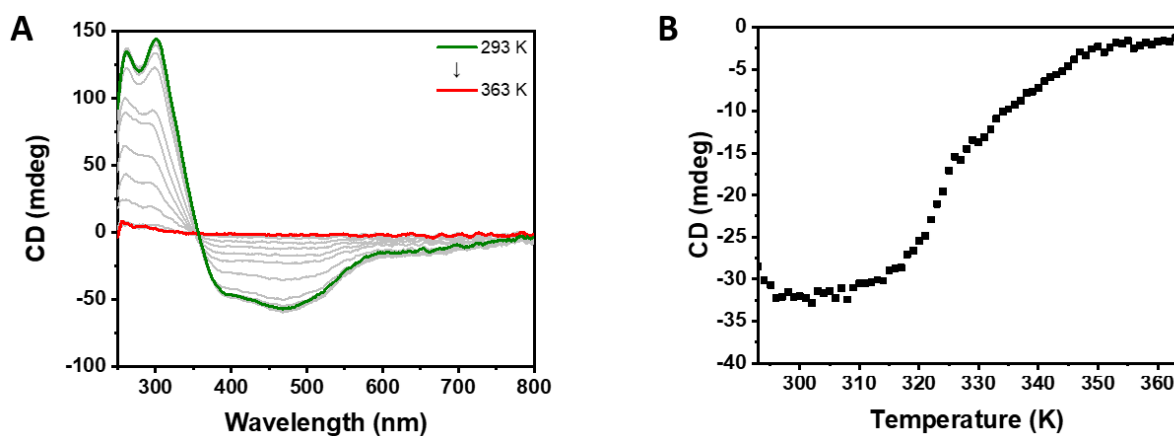


Fig. S7 (A) Temperature-dependent CD spectral changes of **Pt-Sat-C18** (300 μM) upon heating at a rate of 1 K min^{-1} in a mixture of DMSO and H_2O (5:1 v/v). (B) Plots for CD intensity vs. temperatures of **Pt-Sat-C18** at 550 nm.

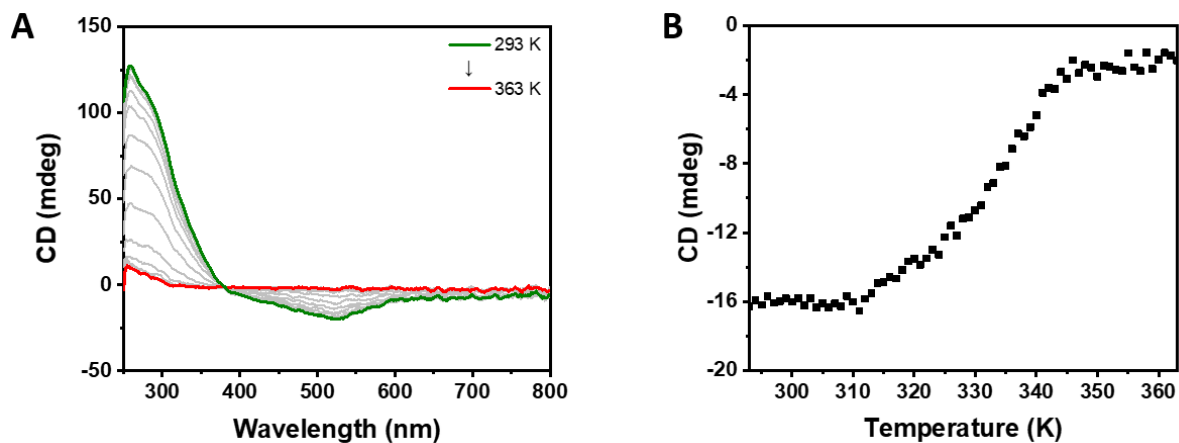


Fig. S8 (A) Temperature-dependent CD spectral changes of **Pt-DA-C25** ($300 \mu\text{M}$) upon heating at a rate of 1 K min^{-1} in a mixture of DMSO and H_2O (5:1 v/v). (B) Plots for CD intensity vs. temperatures of **Pt-DA-C25** at 550 nm.

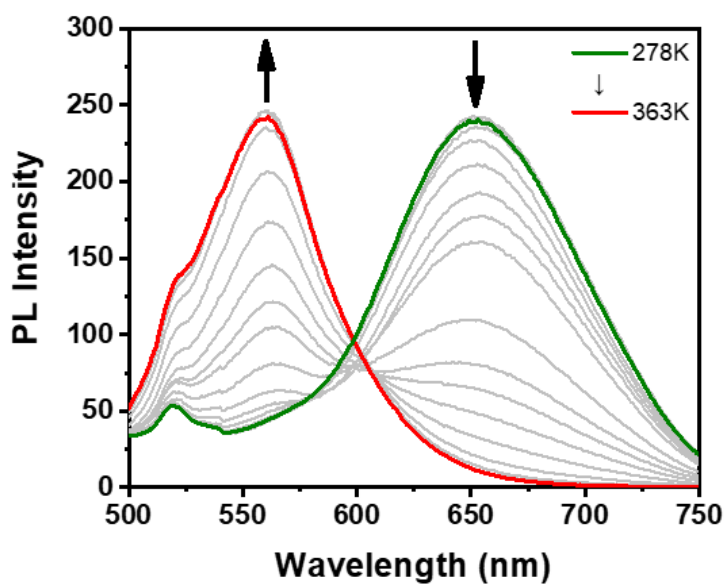


Fig. S9 Temperature-dependent PL spectral changes of **Pt-Sat-C18** ($300 \mu\text{M}$) upon heating at a rate of 1 K min^{-1} in a mixture of DMSO and H_2O (5:1 v/v).

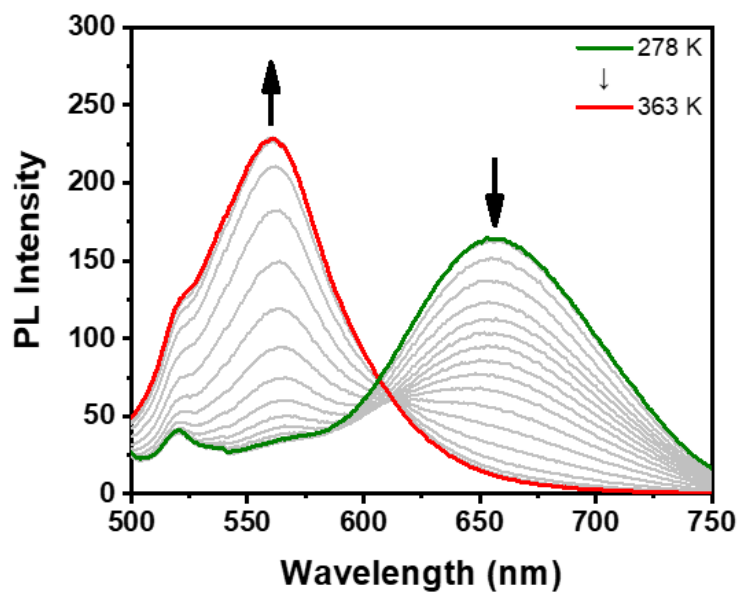


Fig. S10 Temperature-dependent PL spectral changes of **Pt-DA-C25** (300 μM) upon heating at a rate of 1 K min^{-1} in a mixture of DMSO and H_2O (5:1 v/v).

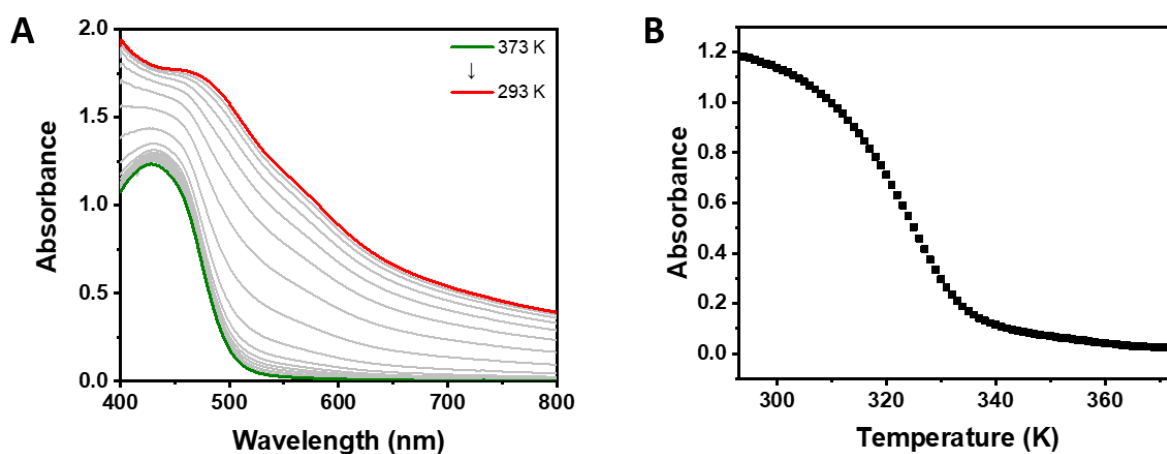


Fig. S11 (A) Temperature-dependent UV-Vis spectral changes of **Pt-DA-C25** (300 μM) upon cooling at a rate of 1 K min^{-1} in a mixture of DMSO and H_2O (5:1 v/v) after UV-irradiation for 30 minutes. (B) Plots for absorbance vs. temperatures of **Pt-DA-C25** at 550 nm.

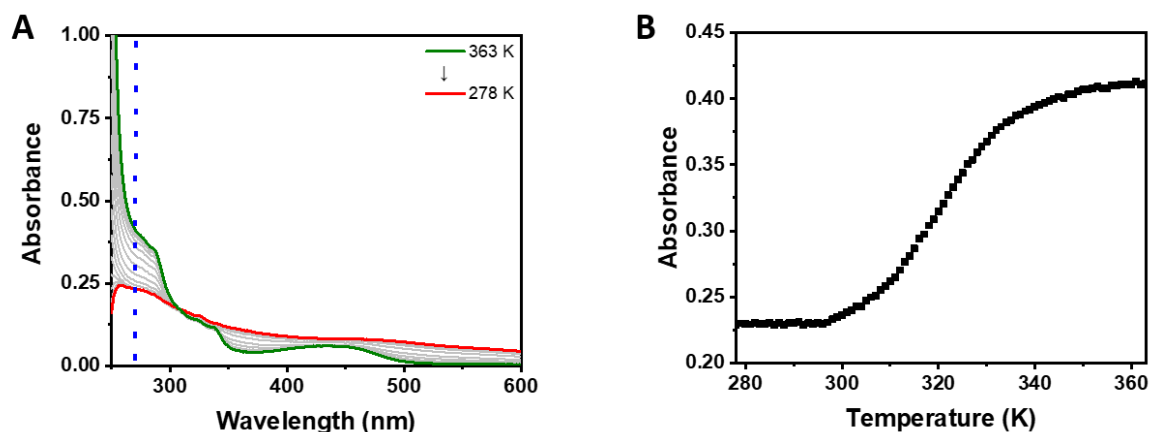


Fig. S12 (A) Temperature-dependent UV-Vis spectra changes of 9:1 ratio of **Pt-Sat-C18** and **Pt-DA-C25** upon cooling at a rate of 1 K min^{-1} in a mixture of DMSO and H_2O (5:1 v/v) after UV-irradiation for 5 min. (B) Plot for absorbance vs. temperature of 9:1 ratio of **Pt-Sat-C18** and **Pt-DA-C25** at 270 nm.

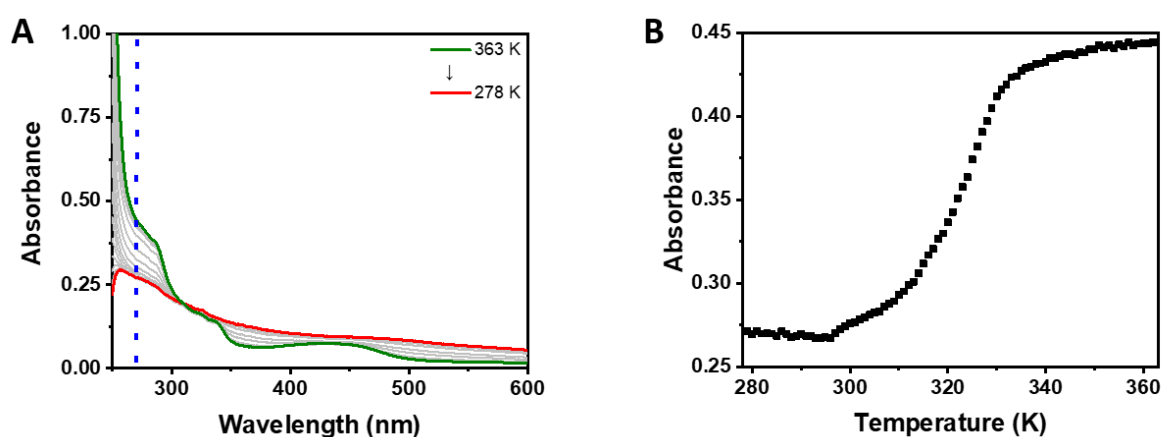


Fig. S13 (A) Temperature-dependent UV-Vis spectra changes of 9:1 ratio of **Pt-Sat-C18** and **Pt-DA-C25** upon cooling at a rate of 1 K min^{-1} in a mixture of DMSO and H_2O (5:1 v/v) after UV-irradiation for 30 min. (B) Plot for absorbance vs. temperatures of 9:1 ratio of **Pt-Sat-C18** and **Pt-DA-C25** at 270 nm.

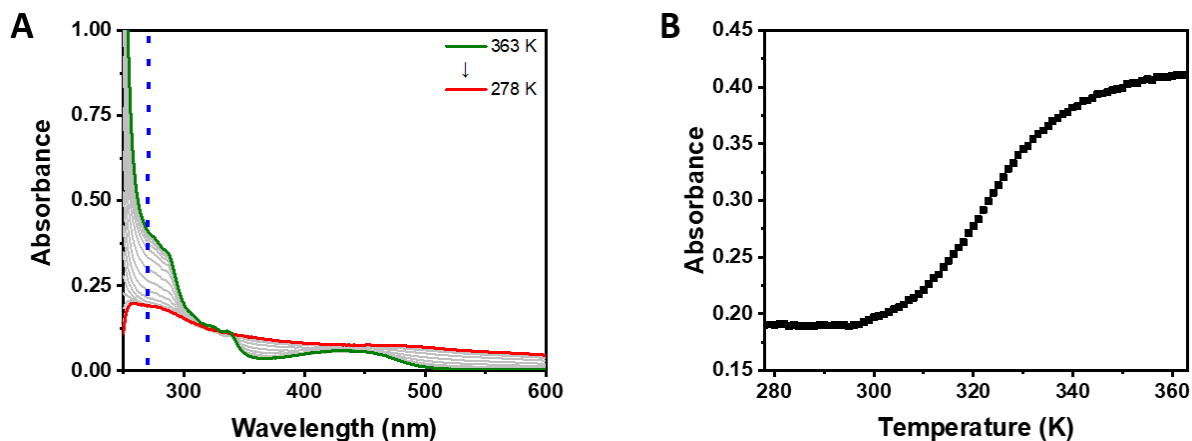


Fig. S14 (A) Temperature-dependent UV-Vis spectral changes of 9:1 ratio of **Pt-Sat-C18** and **Pt-DA-C25** in a mixture of DMSO and H₂O (5:1 v/v). (B) Cooling curve for 9:1 ratio of **Pt-Sat-C18** and **Pt-DA-C25** at 270 nm.

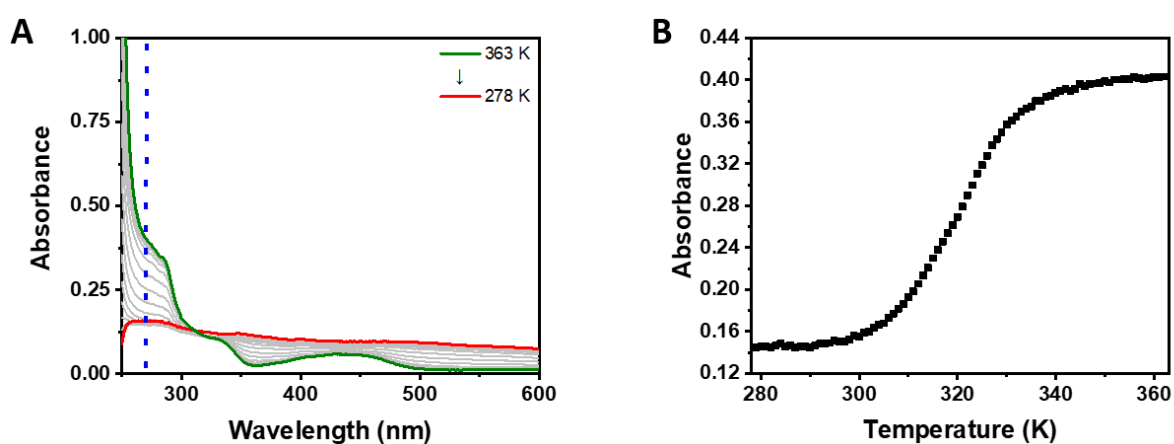


Fig. S15 (A) Temperature-dependent UV-Vis spectral changes of 8:2 ratio of **Pt-Sat-C18** and **Pt-DA-C25** in a mixture of DMSO and H₂O (5:1 v/v). (B) Cooling curve for 8:2 ratio of **Pt-Sat-C18** and **Pt-DA-C25** at 270 nm.

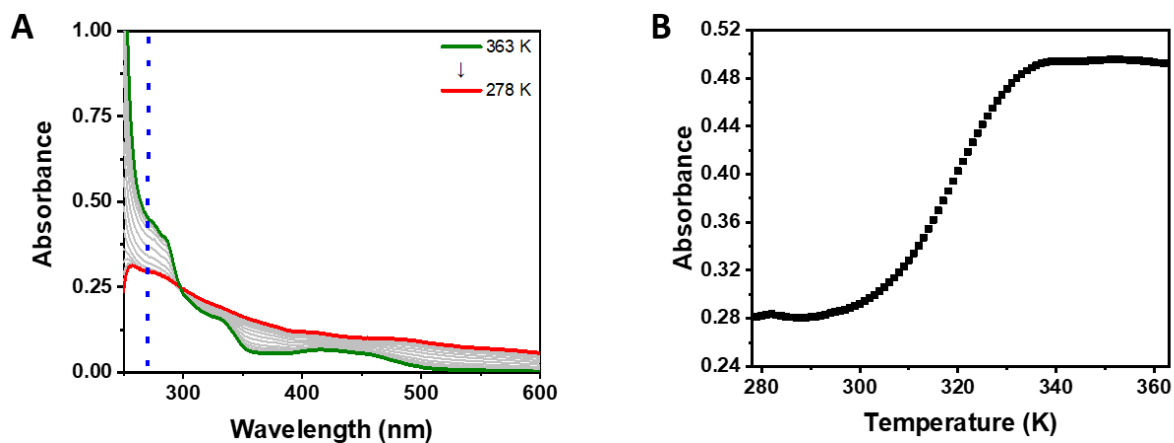


Fig. S16 (A) Temperature-dependent UV-Vis spectral changes of 6:4 ratio of **Pt-Sat-C18** and **Pt-DA-C25** in a mixture of DMSO and H₂O (5:1 v/v). (B) Cooling curve for 6:4 ratio of **Pt-Sat-C18** and **Pt-DA-C25** at 270 nm.

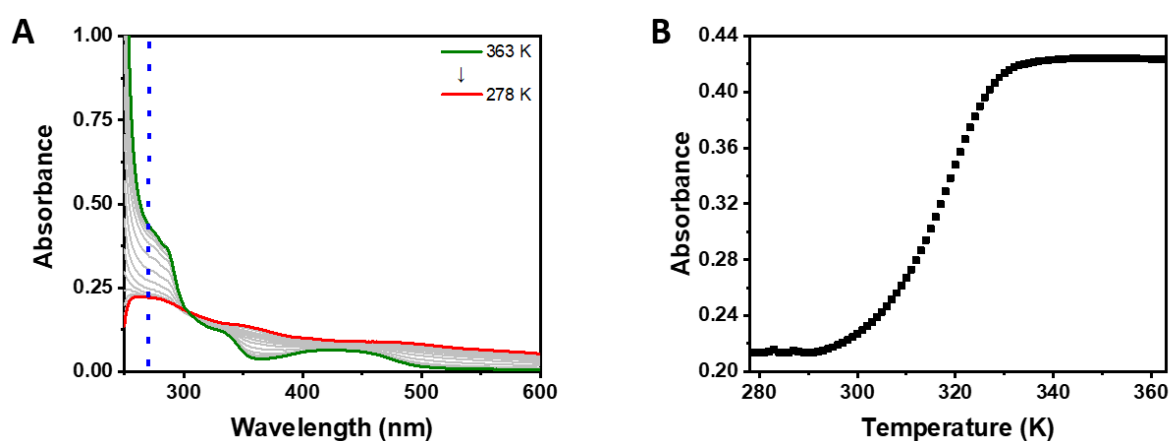


Fig. S17 (A) Temperature-dependent UV-Vis spectral changes of 4:6 ratio of **Pt-Sat-C18** and **Pt-DA-C25** in a mixture of DMSO and H₂O (5:1 v/v). (B) Cooling curve for 4:6 ratio of **Pt-Sat-C18** and **Pt-DA-C25** at 270 nm.

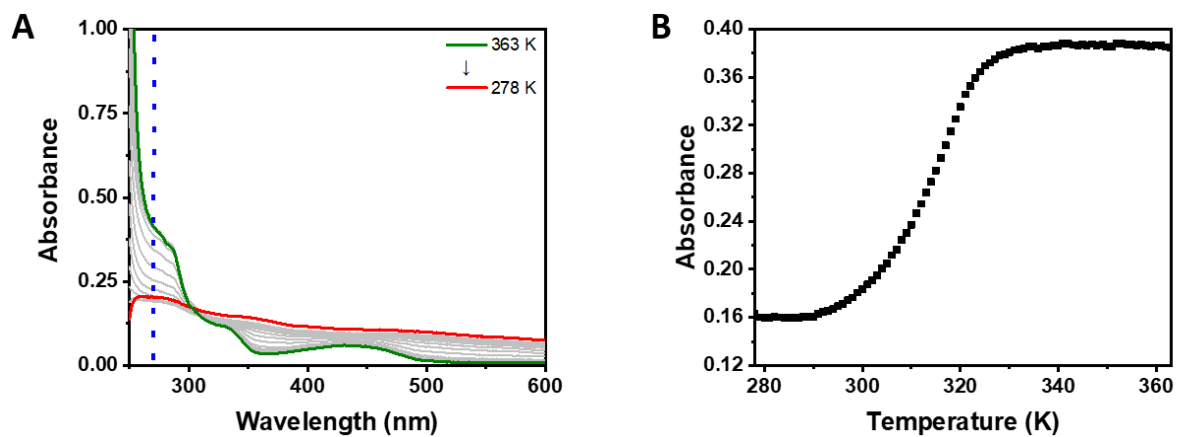


Fig. S18 (A) Temperature-dependent UV-Vis spectral changes of 2:8 ratio of **Pt-Sat-C18** and **Pt-DA-C25** in a mixture of DMSO and H₂O (5:1 v/v). (B) Cooling curve for 2:8 ratio of **Pt-Sat-C18** and **Pt-DA-C25** at 270 nm.

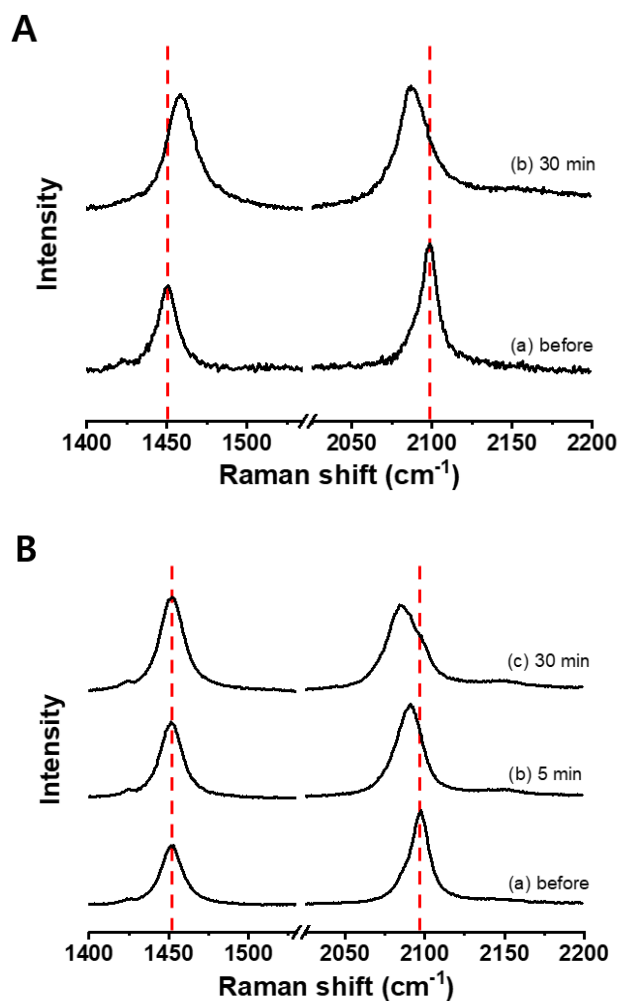


Fig. S19 FT-Raman spectra of (A) self-assembled pure **Pt-DA-C25** (300 μ M) and (B) coassembly of **Pt-Sat-C18** and **Pt-DA-C25** (9:1 ratio) in a mixture of DMSO and H₂O (5:1 v/v) (a) before and (b and c) after UV irradiations.

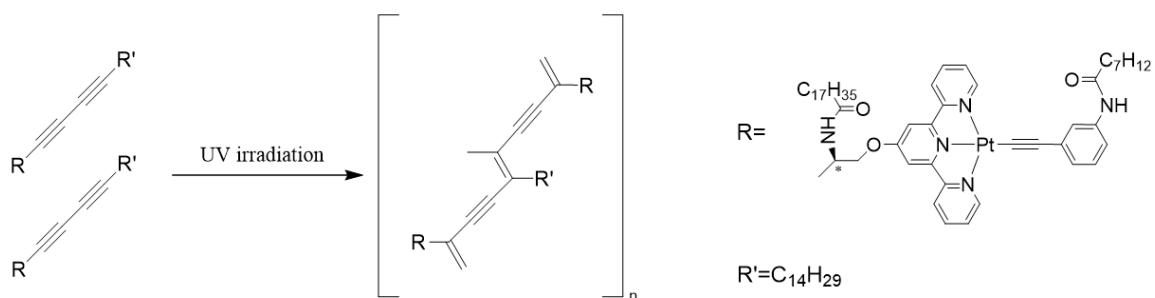


Fig. S20 1,4-Addition polymerization process of supramolecular polymers of **Pt-DA-C25** in mixture of DMSO and H₂O (5:1 v/v) by UV irradiation.

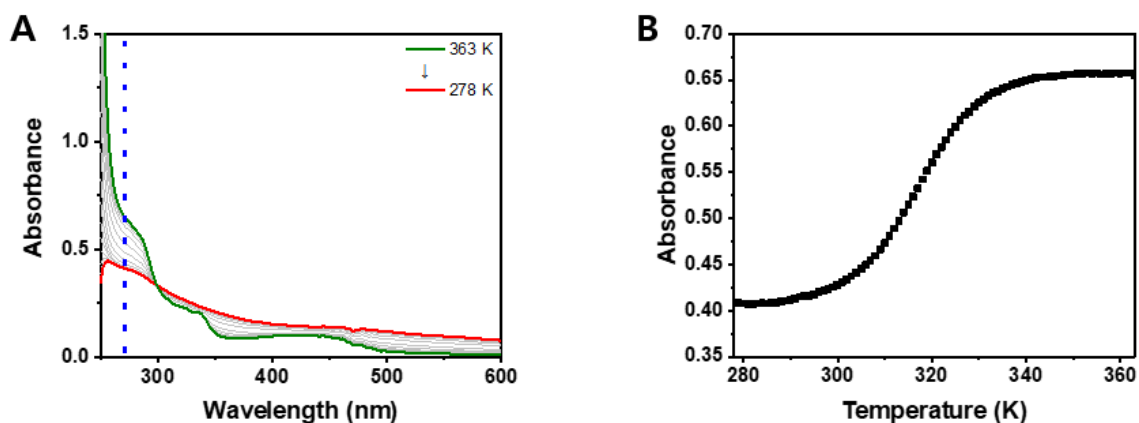


Fig. S21 (A) Temperature-dependent UV-Vis spectra of **Pt-Sat-C18** (200 μM) upon cooling at a rate of 1 K min^{-1} in a mixture of DMSO and H_2O (5:1 v/v). (B) Plot for absorbance vs. temperature of **Pt-Sat-C18** at 270 nm.

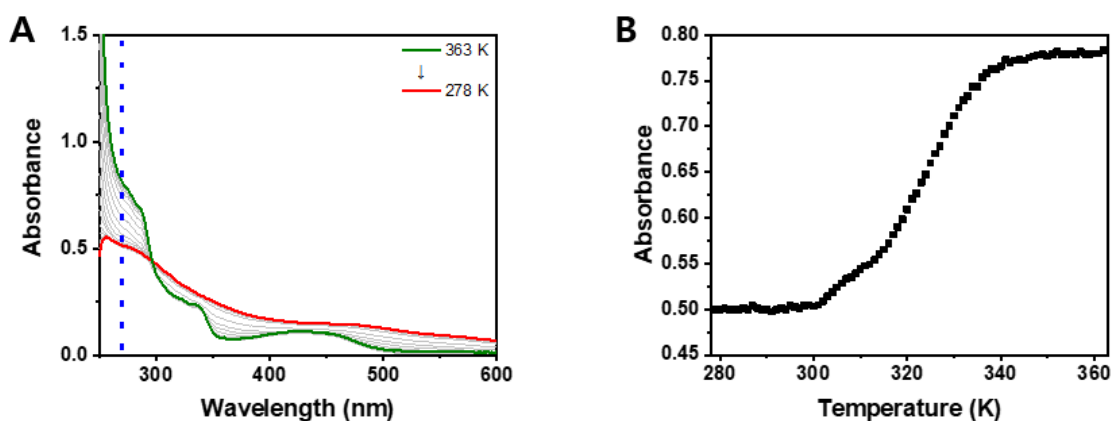


Fig. S22 (A) Temperature-dependent UV-Vis spectra of **Pt-Sat-C18** (250 μM) upon cooling at a rate of 1 K min^{-1} in a mixture of DMSO and H_2O (5:1 v/v). (B) Plot for absorbance vs. temperature of **Pt-Sat-C18** at 270 nm.

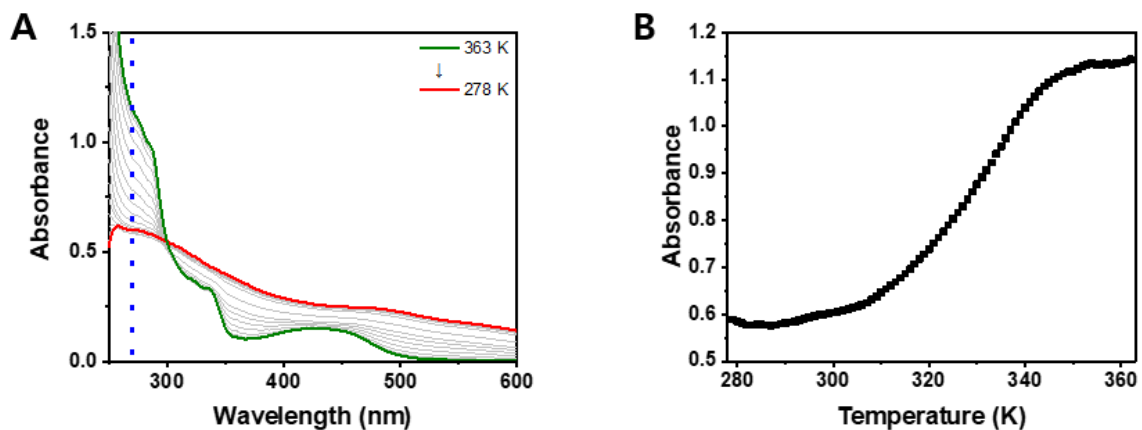


Fig. S23 (A) Temperature-dependent UV-Vis spectra of **Pt-Sat-C18** (350 μM) upon cooling at a rate of 1 K min^{-1} in a mixture of DMSO and H_2O (5:1 v/v). (B) Plot for absorbance vs. temperature of **Pt-Sat-C18** at 270 nm.

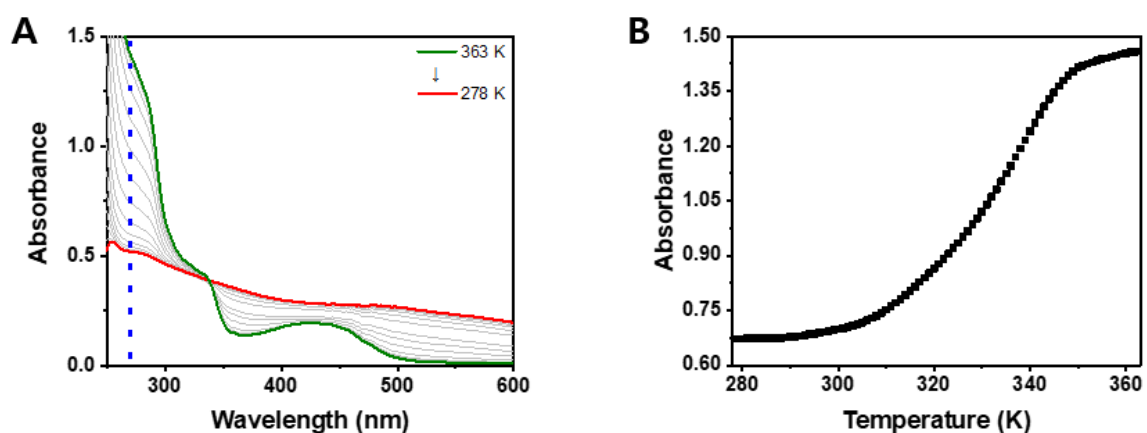


Fig. S24 (A) Temperature-dependent UV-Vis spectra of **Pt-Sat-C18** (400 μM) upon cooling at a rate of 1 K min^{-1} in a mixture of DMSO and H_2O (5:1 v/v). (B) Plot for absorbance vs. temperature of **Pt-Sat-C18** at 270 nm.

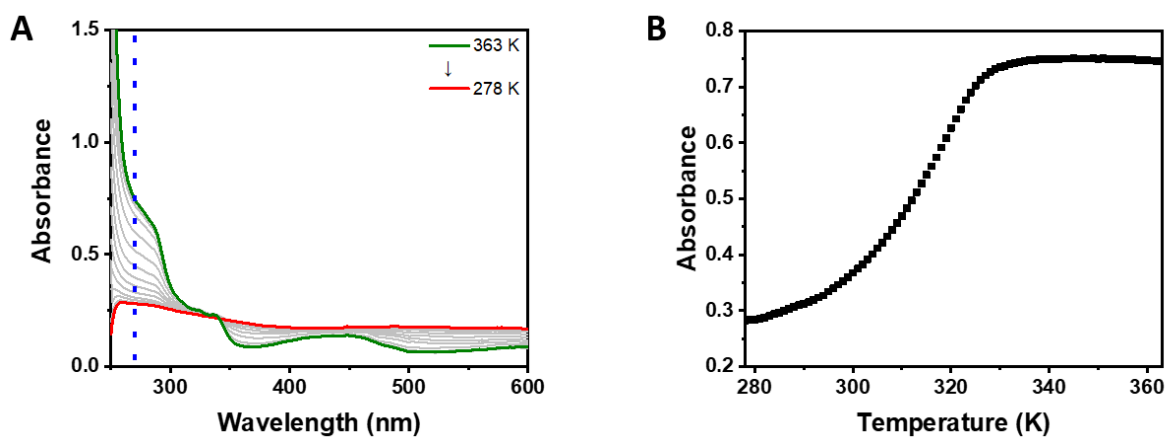


Fig. S25 (A) Temperature-dependent UV-Vis spectra of Pt-DA-C25 (200 μM) upon cooling at a rate of 1 K min^{-1} in a mixture of DMSO and H_2O (5:1 v/v). (B) Plot for absorbance vs. temperature of Pt-DA-C25 at 270 nm.

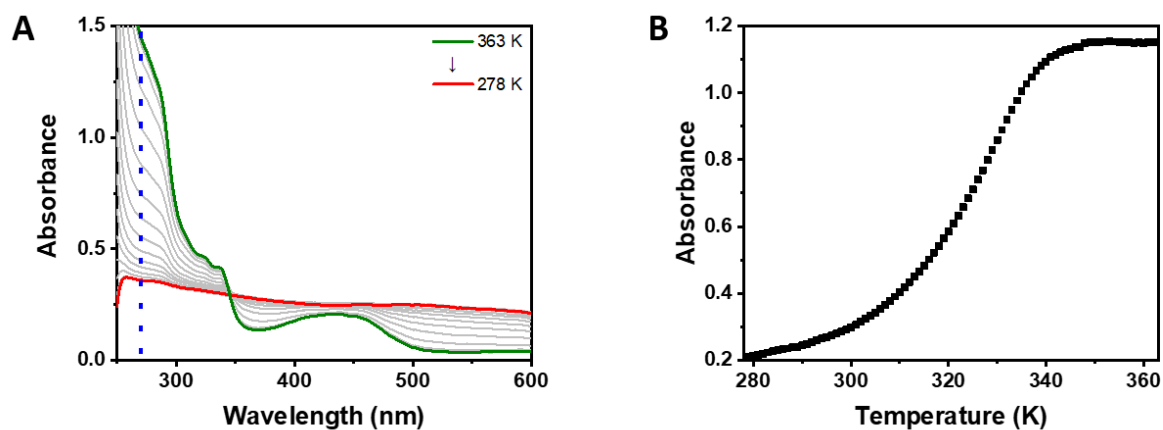


Fig. S26 (A) Temperature-dependent UV-Vis spectra of Pt-DA-C25 (400 μM) upon cooling at a rate of 1 K min^{-1} in a mixture of DMSO and H_2O (5:1 v/v). (B) Plot for absorbance vs. temperature of Pt-DA-C25 at 270 nm.

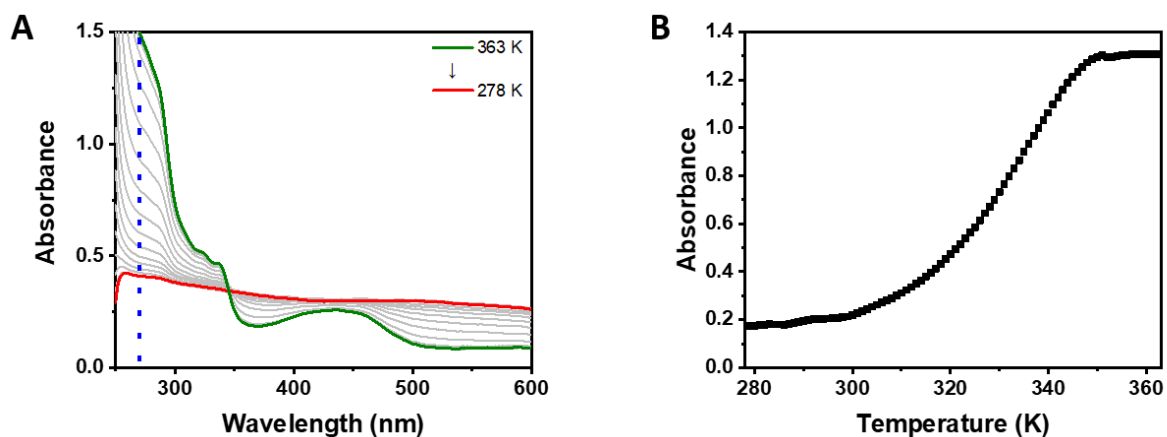


Fig. S27 (A) Temperature-dependent UV-Vis spectra of Pt-**DA-C25** (500 μM) upon cooling at a rate of 1 K min^{-1} in a mixture of DMSO and H_2O (5:1 v/v). (B) Plot for absorbance vs. temperature of Pt-**DA-C25** at 270 nm.

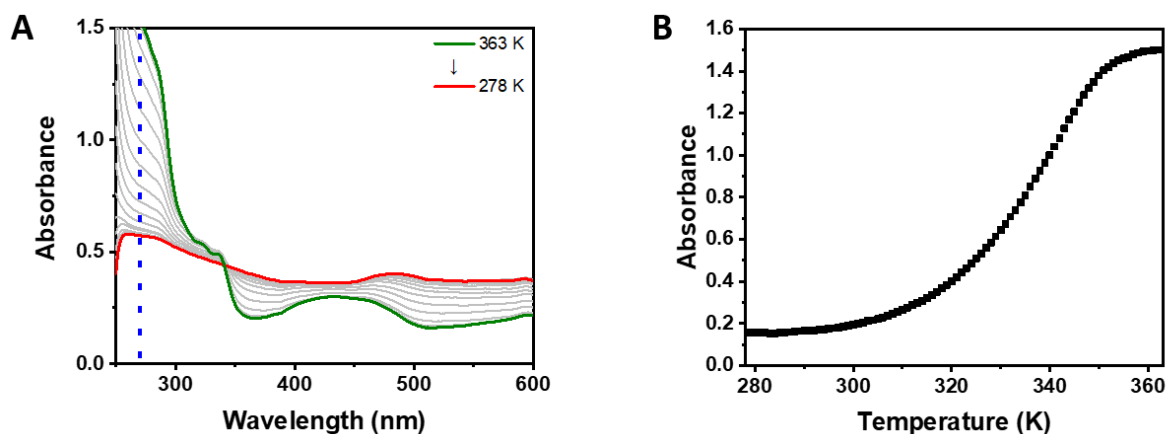


Fig. S28 (A) Temperature-dependent UV-Vis spectra of Pt-**DA-C25** (600 μM) upon cooling at a rate of 1 K min^{-1} in a mixture of DMSO and H_2O (5:1 v/v). (B) Plot for absorbance vs. temperature of Pt-**DA-C25** at 270 nm.

Table S1. Binding constants (K_I) for **Pt-Sat-C18** obtained in a mixture of DMSO and H₂O (5:1 v/v). Thermodynamic parameters obtained from fitting the cooling curves of **Pt-Sat-C18** at different temperatures to isodesmic model. (corresponding to Fig. 5) (K_I : binding constant). Degree of aggregation as a function of the total concentration of **Pt-Sat-C18** (c_T) in mixture of DMSO and H₂O (5:1 v/v) obtained by fitting the apparent absorption at 270 nm to the isodesmic model (equation 2)⁵

Temperature (K)	K_I (M ⁻¹)
328	1.3 x 10 ³
323	2.7 x 10 ³
318	5.4 x 10 ³
313	1.2 x 10 ⁴
308	2.6 x 10 ⁴

$$1 - \alpha_{\text{mono}} = 1 - \frac{2K_I c_T + 1 - (4K_I c_T + 1)^{1/2}}{2K_I^2 c_T^2} \quad (\text{equation 2})$$

Table S2. Thermodynamic parameters for **Pt-Sat-C18** obtained in a mixture of DMSO and H₂O (5:1 v/v).

ΔH (kJ mol ⁻¹)	ΔS (J mol ⁻¹ K ⁻¹)	ΔG (kJ mol ⁻¹)
-126.4	-326.0	-29.3

Table S3. Thermodynamic parameters for **Pt-DA-C25** obtained in DMSO and H₂O (5:1 v/v).

ΔH (kJ mol ⁻¹)	ΔS (J mol ⁻¹ K ⁻¹)	ΔG (kJ mol ⁻¹)	K_e
-43.0	-62.8	-24.3	1.8 x 10 ⁴

Table S4. Thermodynamic parameters for supramolecular copolymers at different ratios of **Pt-Sat-C18** and **Pt-DA-C25** obtained in a mixture of DMSO and H₂O (5:1 v/v).

	ΔG (kJ mol ⁻¹)	K_e	σ
2:8	-19.7	2.8 x 10 ³	1.7 x 10 ⁻²
4:6	-19.1	2.2 x 10 ³	1.7 x 10 ⁻²
6:4	-18.9	2.1 x 10 ³	2.1 x 10 ⁻²
8:2	-16.8	9.0 x 10 ²	4.4 x 10 ⁻¹
9:1	-17.7	1.2 x 10 ³	7.5 x 10 ⁻¹

Table S5. Thermodynamic parameters for **Pt-DA-C25** obtained in a mixture of DMSO and H₂O (5:1 v/v) after UV-irradiation.

Irradiation time	ΔG (kJ mol ⁻¹)	K_e	σ
30 min	-18.8	2.0 x 10 ³	3.0 x 10 ⁻²

Table S6. Thermodynamic parameters for **9:1** ratio of **Pt-Sat-C18** and **Pt-DA-C25** obtained in a mixture of DMSO and H₂O (5:1 v/v) after UV-irradiation.

Irradiation time	ΔG (kJ mol ⁻¹)	K_e	σ
5 min	-18.2	1.5 x 10 ³	6.9 x 10 ⁻¹
30 min	-17.1	9.9 x 10 ²	5.4 x 10 ⁻²

4. Analytical data

4.1 ^1H -NMR and ^{13}C -NMR spectroscopy

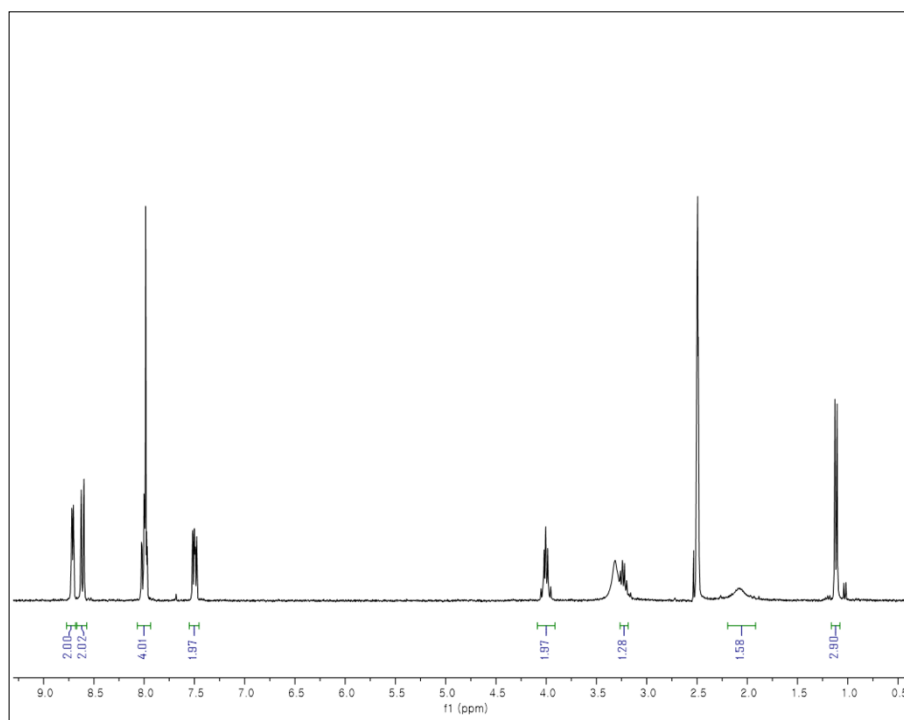


Fig. S29 ^1H NMR spectrum (300 MHz) of **2** in $\text{DMSO-}d_6$ at 298 K.

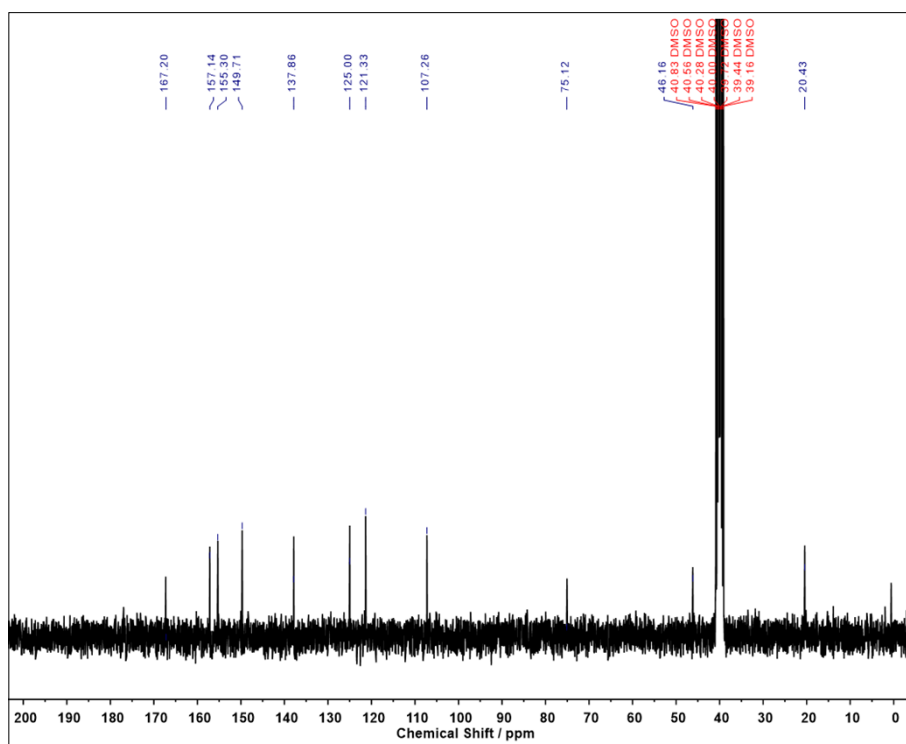


Fig. S30 ^{13}C NMR spectrum (125 MHz) of **2** in $\text{DMSO-}d_6$ at 298 K.

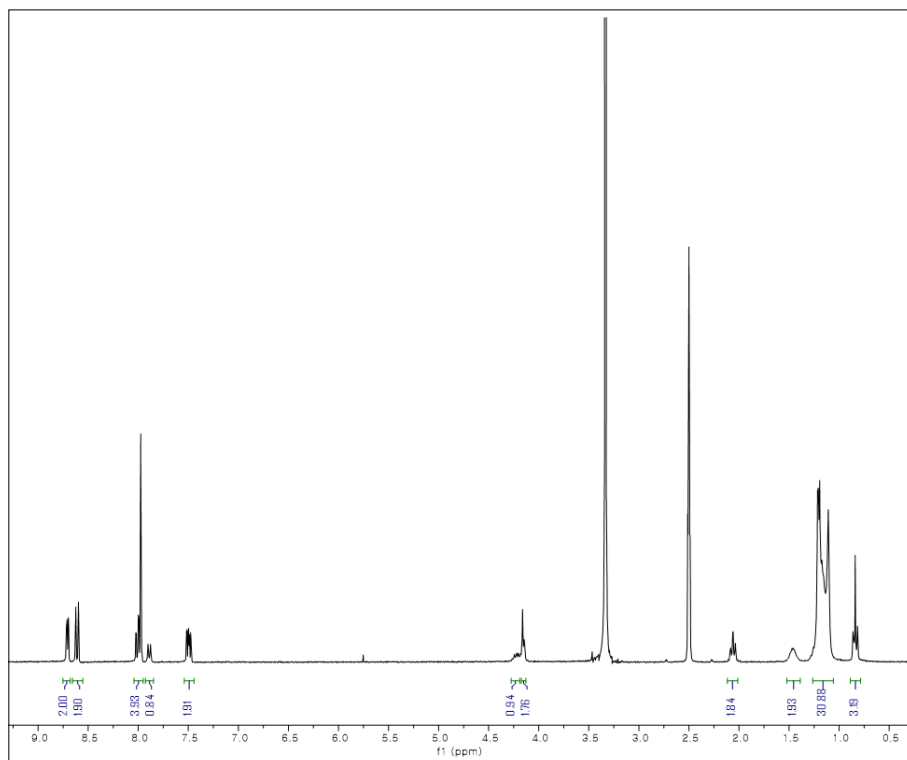


Fig. S31 ^1H NMR spectrum (300 MHz) of **3** in $\text{DMSO-}d_6$ at 298 K.

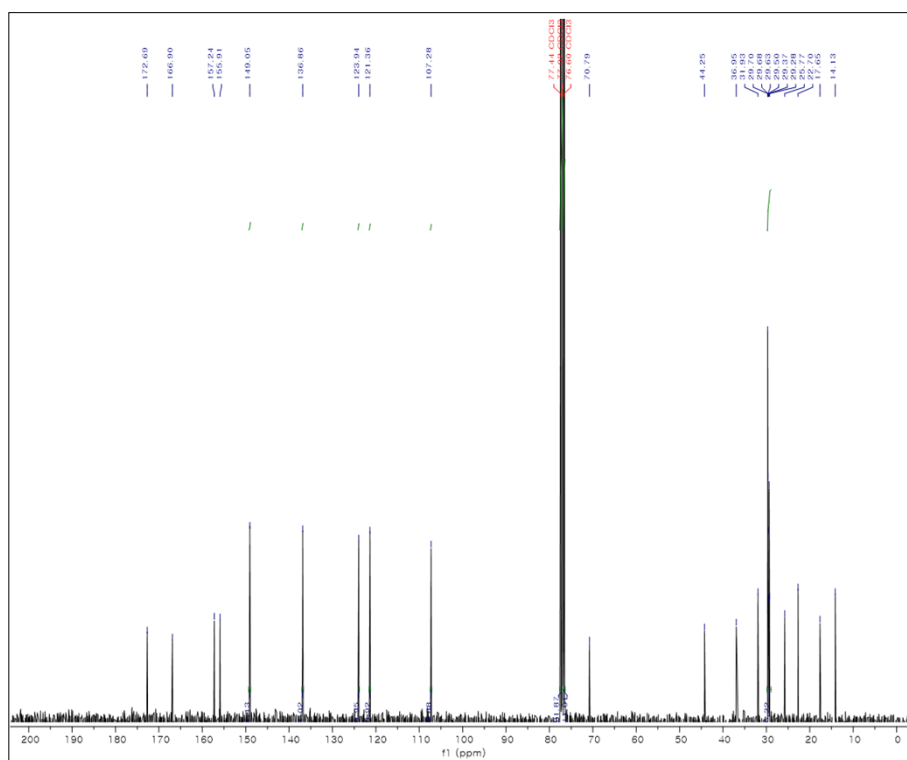


Fig. S32 ^{13}C NMR spectrum (125 MHz) of **3** in CDCl_3 at 298 K.

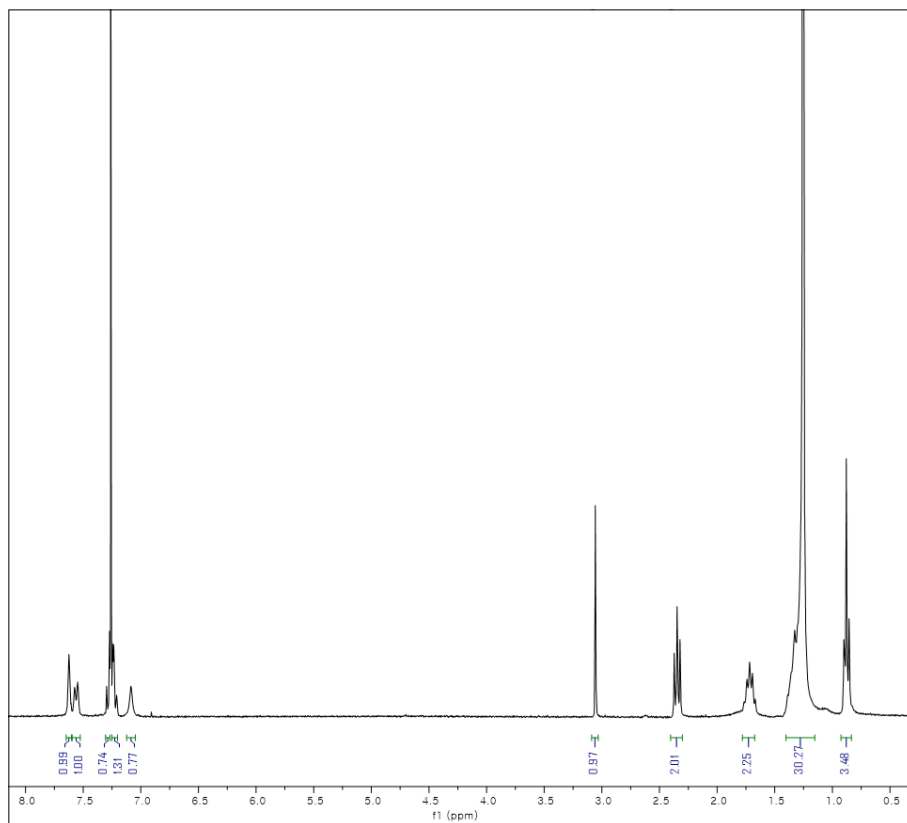


Fig. S35 ¹H NMR spectrum (300 MHz) of **5** in CDCl₃ at 298 K.

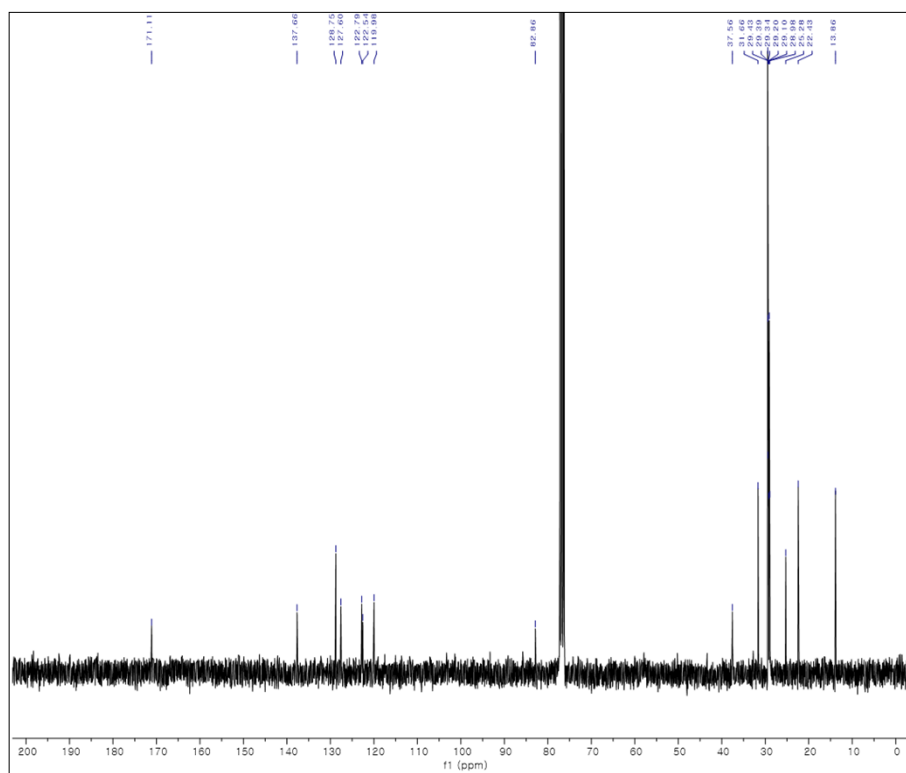


Fig. S36 ¹³C NMR spectrum (75 MHz) of **5** in CDCl₃ at 298 K.

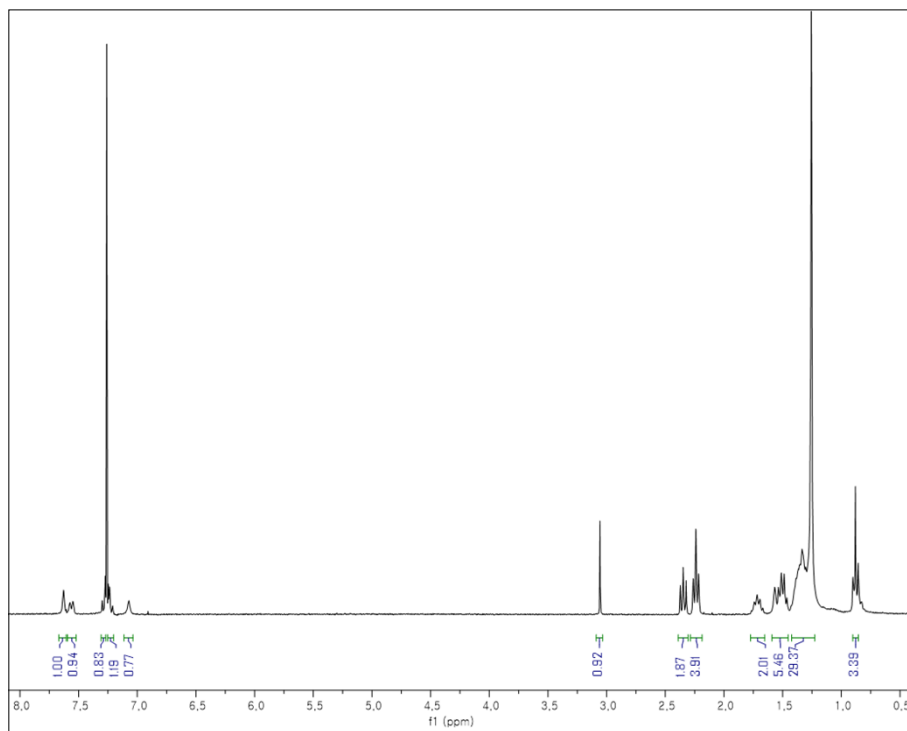


Fig. S39 ¹H NMR spectrum (300 MHz) of **6** in CDCl₃ at 298 K.

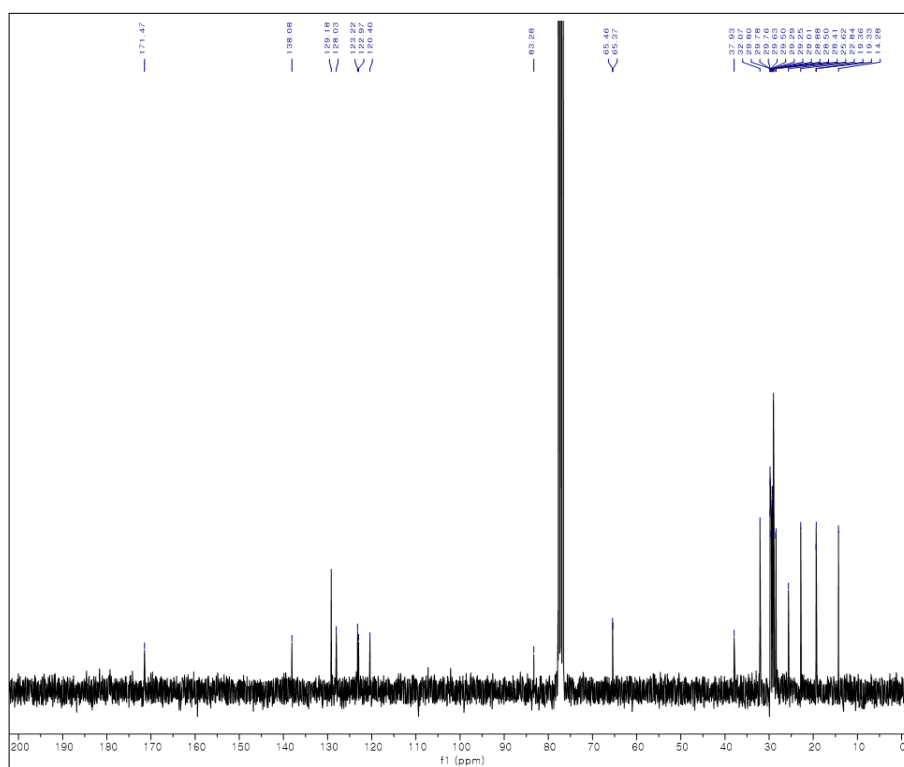


Fig. S40 ¹³C NMR spectrum (75 MHz) of **6** in CDCl₃ at 298 K.

4.2 ESI-MS spectrometry

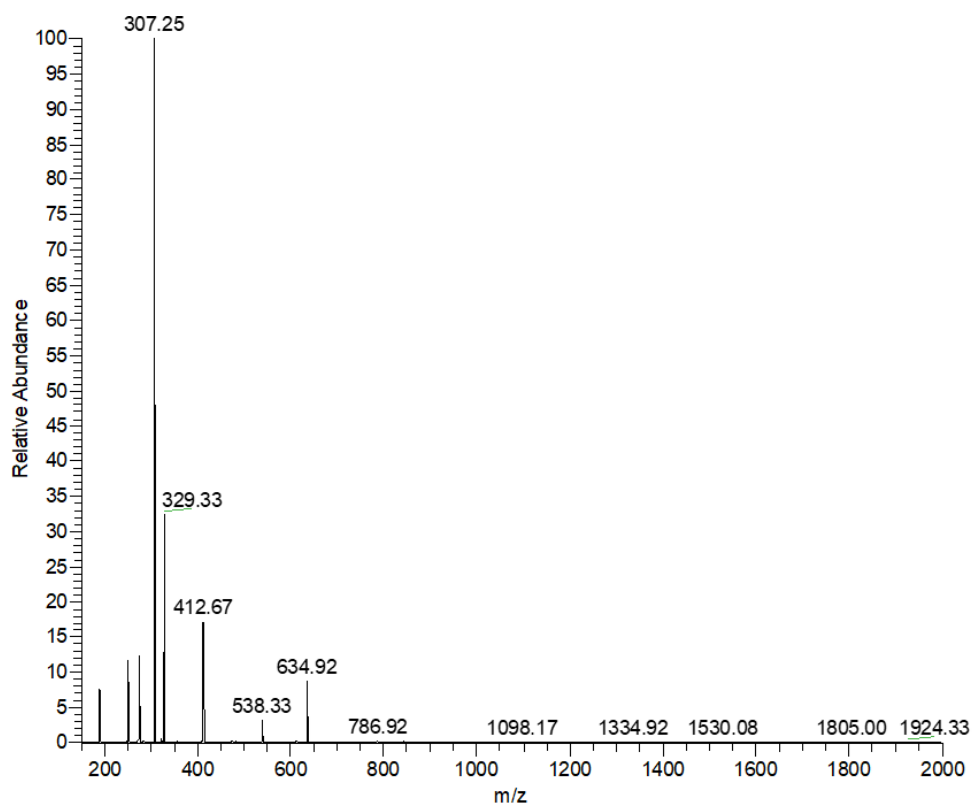


Fig. S43 ESI-MS spectrum of **2** in MeOH.

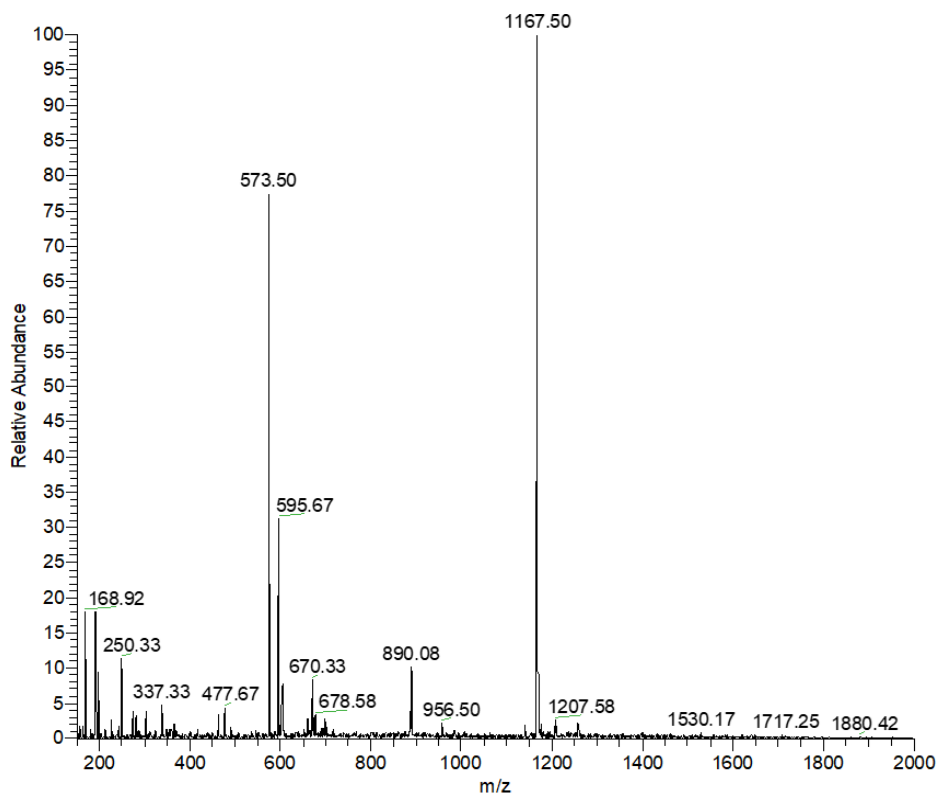


Fig. S44 ESI-MS spectrum of **3** in MeOH.

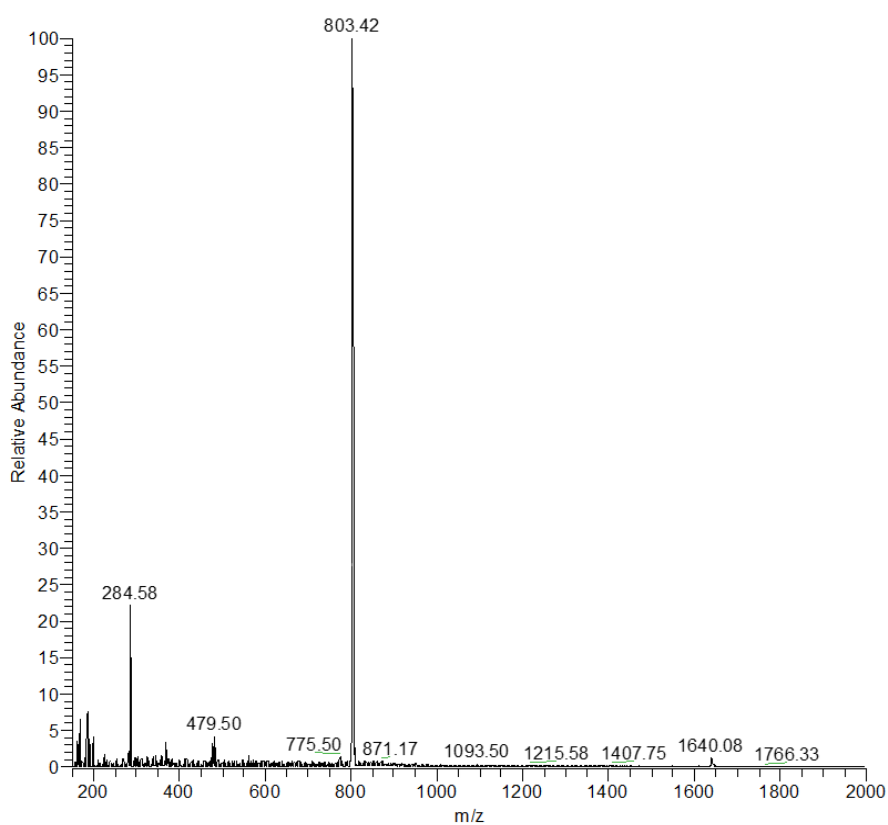


Fig. S45 ESI-MS spectrum of **4** in MeOH.

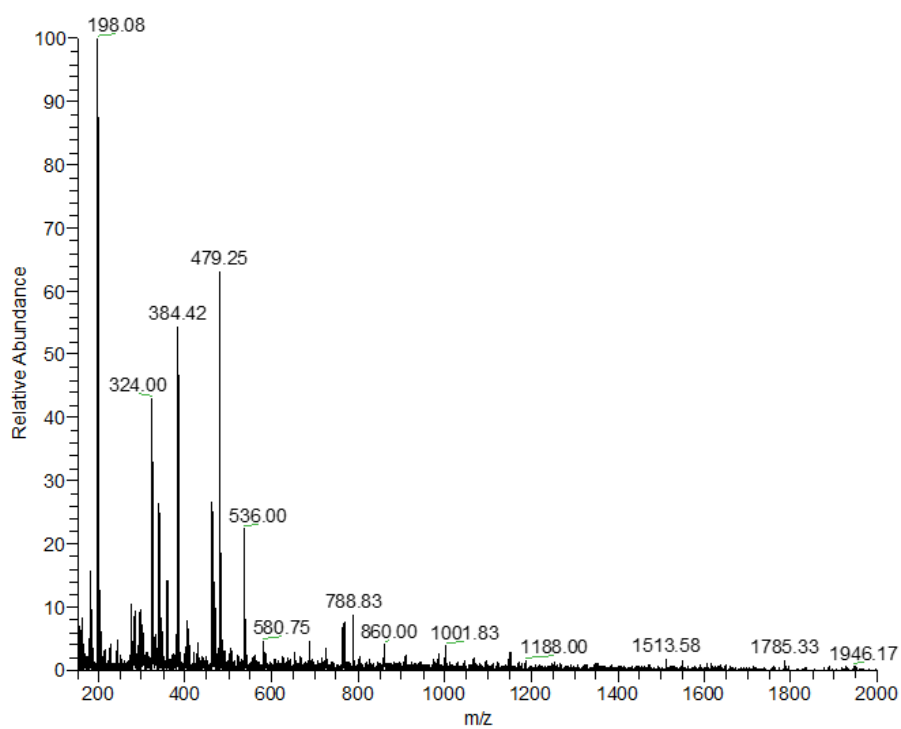


Fig. S46 ESI-MS spectrum of **5** in MeOH.

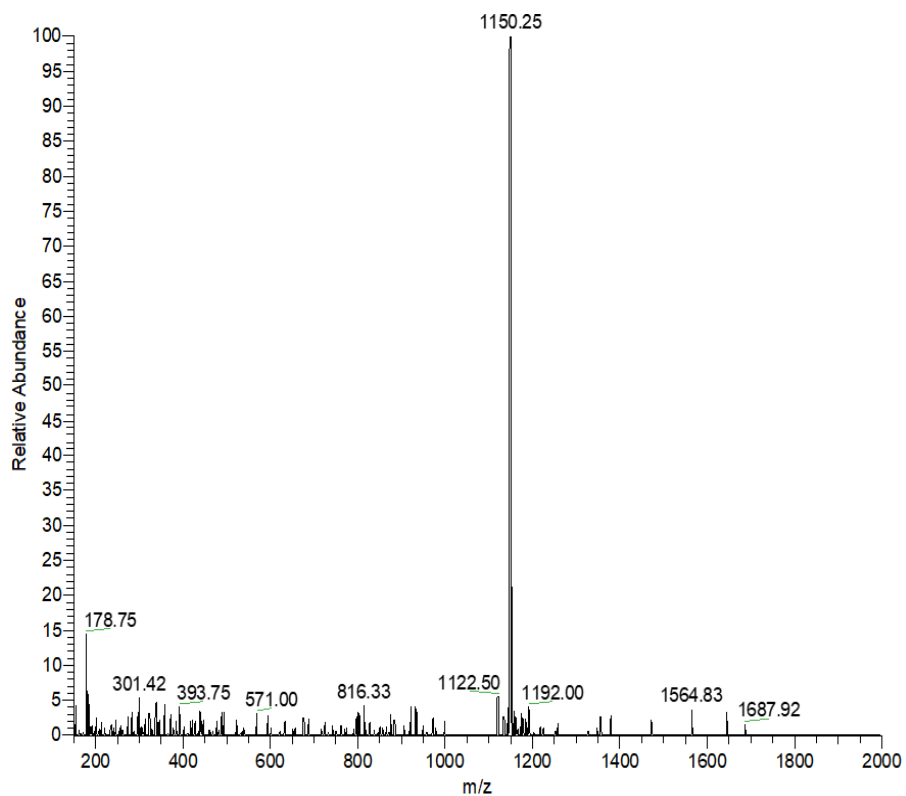


Fig. S47 ESI-MS spectrum of **Pt-Sat-C18** in MeOH.

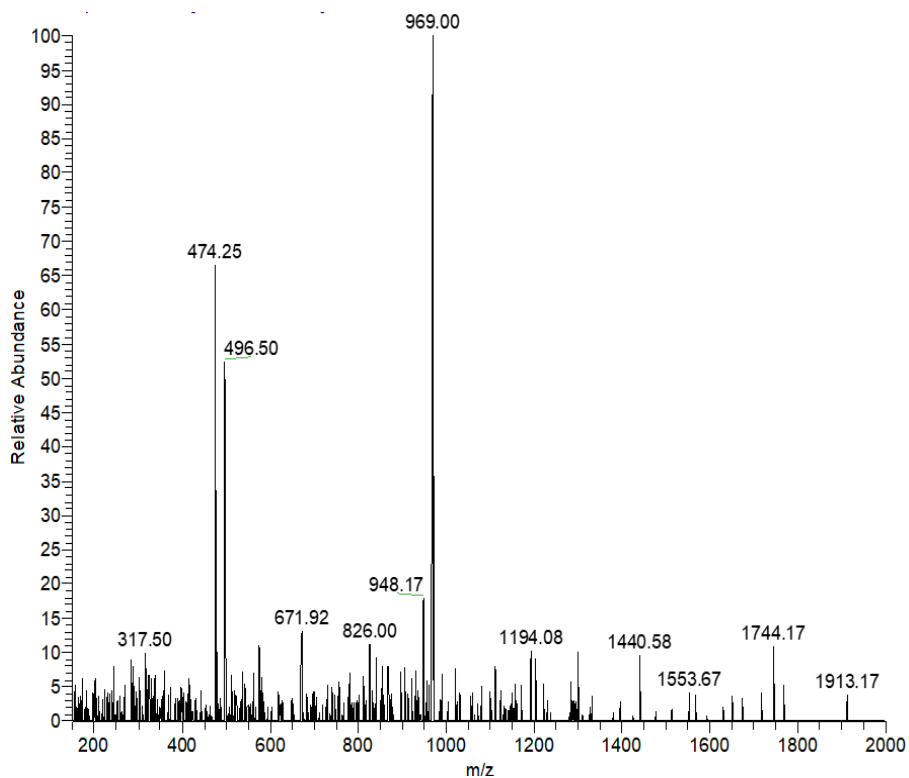


Fig. S48 ESI-MS spectrum of **6** in MeOH.

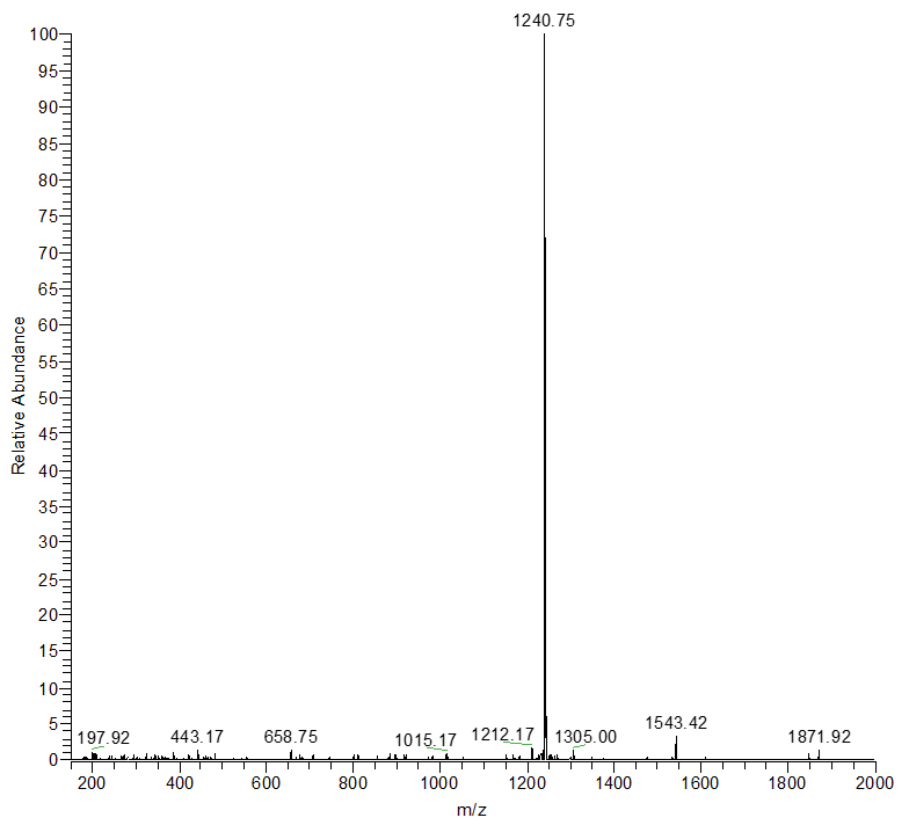


Fig. S49 ESI-MS spectrum of **Pt-DA-C25** in MeOH.

Notes and References

1. H. M. M. ten Eikelder, A. J. Markvoort, T. F. A. de Greef and P. A. J. Hilbers, An equilibrium model for chiral amplification in supramolecular polymers, *J. Phys. Chem. B*, 2012, **116**, 5291-5301.
2. M. M. J. Smulders, M. M. L. Nieuwenhuizen, T. F. A. de Greef, P. van der Schoot, A. P. H. J. Schenning and E. W. Meijer, How to distinguish isodesmic from cooperative supramolecular polymerisation, *Chem. Eur. J.*, 2010, **16**, 362-367.
3. H. Choi, S. Ogi, N. Ando and S. Yamaguchi, Dual trapping of a metastable planarized triarylborane π -system based on folding and lewis acid–base complexation for seeded polymerization, *J. Am. Chem. Soc.*, 2021, **143**, 2953-2961.
4. M. H.-Y. Chan, M. Ng, S. Y.-L. Leung, W. H. Lam and V. W.-W. Yam, Synthesis of luminescent platinum(II) 2,6-bis(N-dodecylbenzimidazol-2'-yl)pyridine foldamers and their supramolecular assembly and metallogel formation, *J. Am. Chem. Soc.*, 2017, **139**, 8639-8645.
5. R. B. Martin, Comparisons of indefinite self-association models, *Chem. Rev.*, 1996, **96**, 3043-3064.